Full-scale in-situ tests on a displacement cast in situ energy pile

Effects of cyclic thermal loads under different mechanical load levels on pile stress and strain

Rafai, Mouadh; Salciarini, Diana; Vardon, Philip J.

DOI
10.1016/j.gete.2024.100606

Publication date
2024

Document Version
Final published version

Published in
Geomechanics for Energy and the Environment

Citation (APA)
Rafai, M., Salciarini, D., & Vardon, P. J. (2024). Full-scale in-situ tests on a displacement cast in situ energy pile: Effects of cyclic thermal loads under different mechanical load levels on pile stress and strain. *Geomechanics for Energy and the Environment*, *40*, Article 100606. https://doi.org/10.1016/j.gete.2024.100606

Geomechanics for Energy and the Environment 40 (2024) 100606

Contents lists available at ScienceDirect

Geomechanics for Energy and the Environment

journal homepage: www.elsevier.com/locate/gete

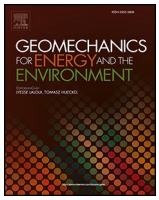

Full-scale in-situ tests on a displacement cast in situ energy pile: Effects of cyclic thermal loads under different mechanical load levels on pile stress and strain

Mouadh Rafai [a,b,*], Diana Salciarini [a], Philip J. Vardon [b,*]

[a] Department of Civil and Environmental Engineering, University of Perugia, via G. Duranti, Perugia 06125, Italy
[b] Faculty of Civil Engineering and Geosciences, Delft University of Technology, Delft 2628CN, the Netherlands

ARTICLE INFO

Editors-in-Chief: Dr. A Ferrari.

Keywords:
Energy pile
Bearing capacity
Full-scale field tests
Multiple mechanical load levels
Thermo-mechanical response

ABSTRACT

Numerous full-scale in situ tests have been conducted to assess the effect of thermal cycles on the pile response. However, those studies investigated the response of only precast and cast in-situ energy piles, with limited focus on the impact of the applied mechanical load on the pile response. This study presents the results of a field test conducted on a new type of energy pile, i.e. a displacement cast in-situ energy pile in multilayered soft soils, subjected to different fixed mechanical loads while undergoing simultaneous thermal cycles. Four tests were carried out, each corresponding to various axial loads ranging from 0 % to 60 % of the pile's estimated bearing capacity. After applying the axial load on the pile head (0 %, 30 %, 40 %, or 60 % of the bearing capacity), the pile was subjected to up to ten thermal cycles. The highest magnitudes of thermal axial strains were observed near the pile top due to the lowest restraint provided by the made ground layer in all tests. Under zero (0 %) mechanical load, the thermal axial strains near the pile head were elastic and recoverable, while residual strain was observed near the toe. Under reasonable working mechanical loads (30 %, 40 %, or 60 %) residual strains were observed near both the pile head and the toe, with higher residual strains observed under higher mechanical loads. The results indicate that the cyclic thermal loadings could induce an increase in the compressive stress in the energy pile, attributed to the drag-down effects of the surrounding soil. The compressive stress induced by drag-down effects counteracts thermally induced tensile stress and thus leads to an insignificant effect on the energy pile during cooling. A limited impact of the shaft capacity was observed and was mainly attributed to the drag-down of the surrounding soil and thermal creep along the pile-soil interface.

Introduction

Energy Geostructures (EGs) are one of the most promising solutions to reduce greenhouse gas emissions in the built environment from new structures, simply by implementing tube heat exchangers in structures such as pile foundations, diaphragm walls, and tunnels, which are in direct contact with the soil, and connecting these structures to a ground source heat pump (GSHP) to provide heating or cooling. Among the different EGs, the use of energy piles is growing rapidly throughout the world, driven by their straightforward implementation and alignment with CO_2 emission reduction policies. Energy piles need to resist and bear the same external mechanical loads as conventional piles, as well as additional thermally induced loads. The heat exchange process induces temperature variations within the soil-structure system, depending on the dynamics of the energy extraction/injection and the dynamics of the heat transfer in the subsurface around these piles.[1–3,51,56] The continuous or intermittent extraction of heat from the soil during winter and its reinjection during summer can generate seasonal, daily, or even hourly temperature variations in both the structures and surrounding soil. These variations, in turn, lead to thermally induced stresses and strains in the soil and the structure. Moreover, the multiple thermal cycles experienced by an energy pile during its operational lifespan can affect its bearing capacity, strain and stress state distributions, displacements, and overall pile performance, which is a topic that so far has received limited attention.

The general thermo-mechanical behavior of energy piles has been extensively investigated through full-scale energy pile tests,[1,4–18] model pile tests,[19–34] and numerical modeling [35–42,52–54] to provide substantial

* Corresponding authors at: Faculty of Civil Engineering and Geosciences, Delft University of Technology, Delft 2628CN, the Netherlands.
E-mail addresses: mouaadrafai@gmail.com (M. Rafai), p.j.vardon@tudelft.nl (P.J. Vardon).

https://doi.org/10.1016/j.gete.2024.100606
Received 1 May 2024; Received in revised form 14 August 2024; Accepted 12 October 2024
Available online 16 October 2024

insight into energy pile behavior, ultimately contributing to the establishment of safe design practices for determining their ultimate bearing capacity in both dry and saturated geotechnical conditions. Although full-scale tests are expensive and time-consuming, the realistic testing conditions provide valuable data for calibrating and validating numerical models and design approaches. In situ tests have shown that the thermal activation of a pile foundation influences its mechanical performance by inducing additional thermal compressive or tensile stresses and axial strains along the pile, depending on whether the pile is heated or cooled, respectively. Specifically, during heating, the mobilized shaft resistance decreases in the upper part of the pile and increases in the lower part, whilst cooling induces the opposite.[4,5,8,17] The results of experimental studies and numerical models indicated an increase in the shaft capacity of the piles due to heating, while the shear strength properties at the pile-soil interface remained largely unchanged. Additionally, the generated stress and strain in the pile can modify the pile's interactions with the surrounding subsurface layers, leading to residual strains and stress due to the drag-down effects, and ultimately changes in bearing capacity.

Cumulative irreversible settlement of the pile head has been observed after thermal cycles in laboratory, full scale and numerical investigations.[16,19,21,39] Faizal et al.[13] showed that the cyclic thermal loading caused a reversible thermal response at pile-soil interface for a bored pile subjected to 16 heating–cooling cycles when the pile head was restrained by a constant building load, approximately equal to 52 % of the estimated ultimate load. Similar results were observed in an unrestrained bored energy pile.[15] Stewart and McCartney[20] performed an end-bearing test on a fully constrained pile, revealing that the thermal axial stress was greater near the toe due to the imposed restriction. Thermal axial strains were found to be similar to the free-expansion thermal strain near the ground surface and decreased with depth; in addition, pile heave was observed during heating. It should be noted that end-bearing piles are usually driven or bored into the ground until they reach a hard layer, such as bedrock or dense sand. Therefore pile tip settlements are likely to be low, and thus pile head settlements will also be limited. However, in regions with thick soft soil layers, displacement of floating energy piles maybe a critical scenario. Ng et al.[19]; and Ng et al.[31] investigated floating energy piles through a series of centrifuge tests. Their findings indicated that such piles experienced more irreversible settlement in lightly over-consolidated clay compared to those in soil with a higher over-consolidation ratio OCR under cyclic thermal loading. Consequently, and logically, they are more susceptible to irreversible ratcheting settlement when compared to end-bearing piles (Ng et al. [31] and Wu et al. [43]). Similar behavior was reported by Zhao et al.[32] of a laterally-loaded pile. Jiang et al.[16] investigated the thermo-mechanical behavior of driven energy piles under different mechanical loads, their results showed that cooling-recovery cycles developed an elastic–plastic pile response at a specific mechanical loading level, with cooling-induced settlement being several times that of mechanical load-induced settlement. Since this study focused on the pile head displacements, the strain and stress measurements were not reported.

Kong et al.[18] reported that residual strains, stresses, and settlements developed during the thermal cycles, even when the temperature was fully recovered. Jiang et al.[59] investigated a long floating energy pile during short-term thermal cycles (up to three cycles of cooling–natural heating and heating–natural cooling) under a constant mechanical load. Their results showed that heating induced a significant additional axial force, which could reach up to four times that of the pile under purely mechanical loads. In contrast, cooling reduced the stress initially generated by the applied mechanical load. The increase or decrease of the axial load depends on the magnitude of the temperature change.[59]

Nguyen et al.[27] reported that the irreversible settlement of the pile head stabilized when the pile loading was approximately 20 % and 40 % of the estimated bearing capacity of the pile, while at 60 % it continued to increase after 20 cycles, again the strain and stress measurements were missing. Note that in their study (Nguyen et al. [27]), a small-scale aluminum tube pile was installed in dry sand with a relative density of 50 % and the reported results can be considered only as quantitative data, any extrapolation of these results to field applications should be cautiously treated. For this reason, they suggested conducting such a testing program on full-scale energy pile.

More recently, Golchin et al.[33] and Rafai et al.[34] investigated the thermally induced shear creep of the soil–structure interface using temperature-controlled shear boxes under thermal cyclic loading while mechanic loads were held constant (effective and shear stresses), representing loading/thermal conditions representative of floating energy piles. The results showed that the thermally induced shear displacement depends on the applied normal and shear stresses (which relate to the normal stress from the soil and the pile head load respectively) and soil type and density. Under higher mechanical loads (equivalent to higher pile head loads), higher shear displacement was observed due to thermal cycles. Previous studies have shown that the longer-term behavior of energy piles may induce different phenomena: i) By affecting the properties or causing volume changes of the surrounding soils, drag-down or uplift of the surrounding soils can be induced;[11,16,18] ii) Modifying the stress state at the soil-structure interface and pile tip due to the thermo-mechanical loads may induce plastic strain and thermal shear creep in the long-term,[26–28,33,34] cumulative irreversible settlement being greater under higher constant head loads,[16,18,21] and ratcheting effects in heavily-loaded piles undergoing thermal cyclic.[21,26,32–34,37,50] It has been observed that the thermal-induced deformation at pile-soil interface and pile head can be intensified under cyclic changes in pile temperature depending on the applied mechanical load.[16,27,28,33,34]

According to the literature, full-scale tests are primarily focused on energy piles subjected to either a constant mechanical load and long-term thermal cycles[11,13,15,17] or different constant mechanical loads and short-term thermal cycles[16,18] (up to five thermal cycles). However, the impact of different mechanical loads and long-term thermal cycles - critical factors in design - remains poorly understood, with only limited data available from full-scale tests in diverse soil conditions. Furthermore, the behavior of energy piles in soft soils is limited to floating energy piles.[16,59] Further field data on semi-floating energy piles in multilayered soft soil are required. Although the aforementioned full-scale studies have shed light on several aspects of the fundamental mechanism governing pile behavior under thermo-mechanical load, the existing energy piles type are limited to pre-cast driven energy piles,[10,16] cast-in situ energy bored piles[14,15,17] and belled energy piles.[18] In this study, a displacement cast in situ Fundex pile (hereafter referred to as a displacement cast in-situ pile) has been used. Displacement cast in situ piles offer several advantages, including convenient construction, simple manufacturing, vibration-free, and low noise and cost. Moreover, they can be easily used and installed under different geological conditions. Their installation method uses an auger tip (alongside a temporary casing for installation) that displaces soil laterally, thereby densifying and compacting the surrounding ground. Displacement piles may be particularly advantageous in regions where soft soils are dominant, such as the Netherlands. This paper presents results from a series of full-scale field tests of a semi-floating energy pile in soft soil under cooling–natural heating cycles (up to ten) with an average temperature variation of approximately 10 °C while the mechanical load was held constant. This can simulate multiple years of seasonal GSHP operation.[27,60] Various tests have been performed under different loads of 0, 30 %, 40 %, and 60 % of the estimated pile bearing capacity. The paper contains first a description of the field test and the experimental program. The monitoring data are then presented and analyzed to elucidate the effects of thermal cycles under different loads on energy piles. The potential effects of the applied load on the thermally induced strain and stress as well as the effects of thermal cycles on the shaft capacity are discussed.

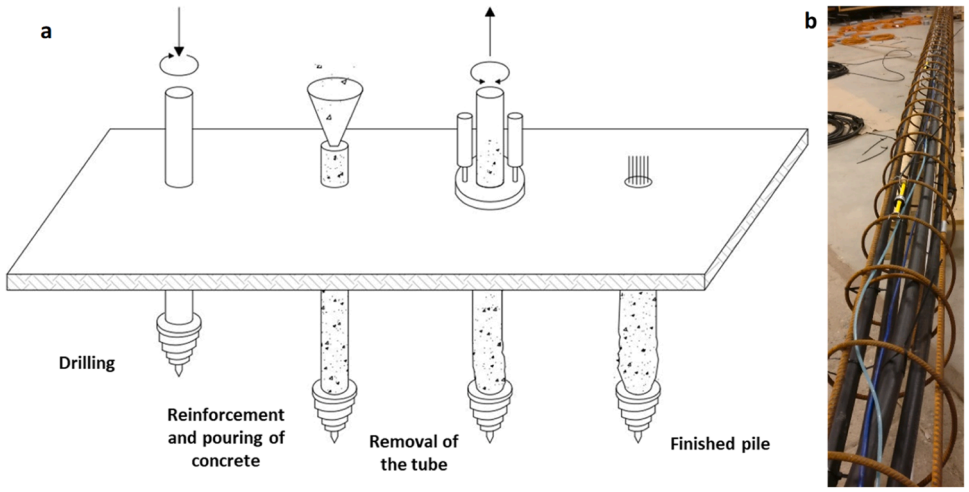

Fig. 1. (a) Installation phases of the Fundex energy pile (modified from https://www.fundex.nl/en/); (b) reinforcement cage with the heat exchanger loops and monitoring system.

Description of the field test

Energy pile and instrumentation

A Fundex displacement pile was installed at Delft University of Technology in Delft, the Netherlands, as an energy pile with a double-U-tube, and instrumented such that thermally induced displacements, strain, and stress could be measured in conditions characterized by soft soils and a water level close to the ground surface. Mechanical and thermal loading were controlled, such that the measurements could be related to the driving mechanisms. Schematic views of the installation phases of the energy pile are shown in Fig. 1. In the drilling phase, a steel casing/tube with a conical auger tip attached to its end is rotated clockwise and pushed down into the soil. As the tip penetrates the ground it displaces the soil laterally, effectively compacting the surrounding area. After reaching the desired depth, a reinforcement cage containing the heat exchanger loops (Fig. 1(b)) is installed into the casing, which is subsequently filled with concrete. The conical tip is then released from the casing, then the casing is removed. The sacrificial tip forms an expanded pile tip. The pile's toe was positioned at a depth of 10.3 m below the ground surface, representing the top of the tip used in the construction, with a shank diameter of 380 mm and a tip diameter of 400 mm.

Two high-density polyethylene (HDPE) pipe closed loop heat exchangers in a "U" configuration (U-loops), with an internal diameter of 28 mm and a quoted surface roughness of 0.007 mm, were attached to the inside of the reinforcing cage of the pile (as shown in Fig. 1(b) and Fig. 2). The horizontal spacing between the loops was approximately 112 mm. Twelve Vibrating Wire Strain Gauges (VWSGs) with integrated thermistors were fixed at different depths. VWSGs were placed symmetrically in two strings, on opposing sides of the pile cage, in the gaps between pipes. Vertical strains were measured at six levels along the pile on two sides and the average of each pair of gauges was considered in the calculation.

The locations within the cross-section and along the pile depth are indicated in Fig. 2. The locations along the pile depth refer to the average depth of the two strain gauges, i.e. the position of the thermistor. The strain gauges were used to assess the effects of the thermo-mechanical load on the pile shaft. Pile head movements were measured using a linear variable differential transformer (LVDT) with an integrated thermistor to monitor the air temperature. This LVDT, with an accuracy of 0.001 mm, was placed in contact with the top of the pile (Fig. 2).

A tank container with a volume of 26,000 L was used to provide the dead weight for static load testing and was utilized as the heat source/sink (see Fig. 2). When filled with water, this provides a maximum weight of up to 33 tons (323.7 kN).

Mechanical loading at the pile head was applied by means of a hydraulic jack that was used to develop a compressive force on the pile head, coupled with one load cell placed between the jack and the frame to record and control the applied loads (see Fig. 2). A ground source heat pump (GSHP) was connected to the pile and the tank was used to provide the thermal load by heating the tank while cooling down the pile and vice versa. The heat exchange fluid used in the GSHP system was a mixture of 30 % monoethylene glycol and 70 % water by volume. All the instrumentation was connected to a data logger system to record continuous measurements along the pile shaft with a time interval of one minute.

Soil properties

A preliminary geotechnical characterization was undertaken by drilling an approximately 13-m-deep borehole at the test pile location and cone penetration testing (CPT). The cone (qc), sleeve (fs) resistances and pore water pressure (u) results are shown in Fig. 3. The soil profiles and the groundwater location are shown on CPT results in Fig. 3. The test site features soil conditions typical of the western Netherlands. The surface layer is a shallow made ground, underlain by 2.1 m of very soft highly organic clay (i.e. peat) (qc ≈ 0.3 MPa). With increasing depth, a very soft silty sand layer ranges from 4.1 m to 7.6 m (qc ≈ 3 MPa), followed by a 1 m thick soft clay (qc ≈ 0.8 MPa). Underneath this lies a layer of slightly firmer sand extending from 8.7 m to 12.0 m, with qc values of 6–10 MPa. The pore pressure increased at the depths of 2.1 m to 4.1 m up to 0.2 MPa and 7.6 m to 8.7 m up to 0.45 MPa demonstrating the presence of low permeability peat and clay respectively, while in the other soil layers, the pore pressure was about 0.1 MPa (Fig. 3). The pile penetration depth of 10.3 m means that it was embedded into the sand layer. The initial ground temperature was ~12°C below the depth of 4 m.

Experimental scheme

Prior to the execution of thermal and thermo-mechanical response tests, a pressure test of the installed piping, manifold, connections, and heat pump was carried out to ensure the system can adequately generate and sustain the hydraulic pressure required for the flow. The testing schedule, as shown in Table 1, includes six testing phases: Two mechanical load tests (before and after the thermo-mechanical tests), a

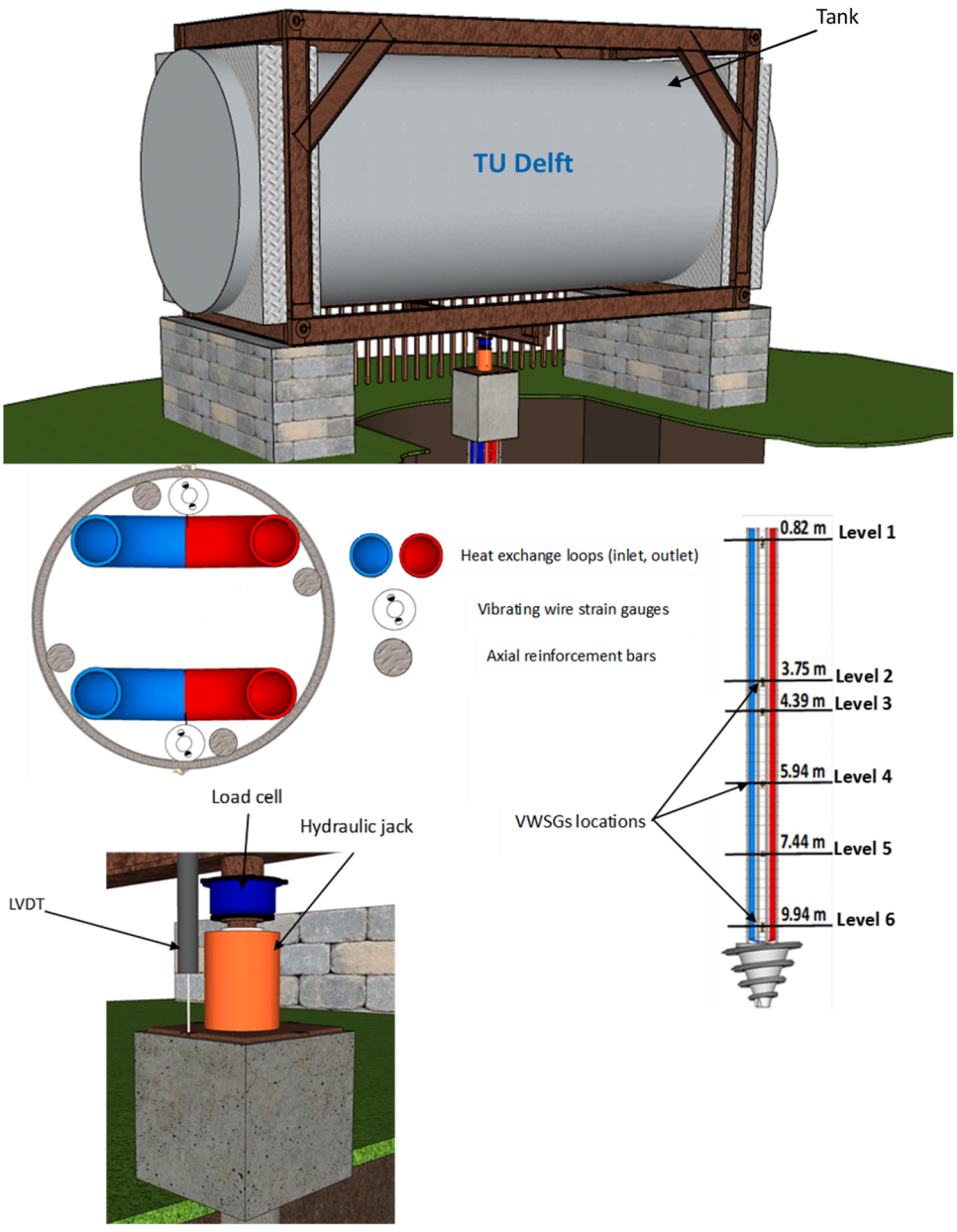

Fig. 2. Schematic of the energy pile including instrumentation and their locations.

thermal test, and three periods of thermo-mechanical testing at different mechanical loads. The predicted bearing capacity was calculated to be 353 kN. Note that this value excludes the shaft resistance of made ground and peat layers. In the first phase, the pile was loaded up to 0.6 Q_{max} (60 % of the estimated bearing capacity) with increments of 0.1 Q_{max} (10 %), each loading steep was maintained for at least 60 min. Afterwards, the pile was unloaded. For the mechanical tests, incremental loading according to the procedure recommended by the Dutch code for static axial loading of piles[44] was adopted. According to the adopted standards,[44] the mechanical creep (k) is defined as the change in pile head displacement over the last 15 min of a load step divided by the log-time. When the mechanical creep is less than 0.75 mm/15 min, then the mechanical load can be increased. During the second phase, a free-expansion test was conducted with no load applied to the pile. In this particular test, the pile was subjected to two cooling-natural heating thermal cycles, with an average temperature variation of approximately 10 °C. During the third phase, in the thermo-mechanical tests, the pile was first loaded up to a defined value (30 %, 40 % or 60 % of the estimated bearing capacity). The target axial load was then maintained for a duration ranging from 10 to 16 h to minimize the creep effects, and then up to 10 thermal cycles of cooling-natural heating were applied. Once the target temperature was reached, it was sustained for 12 h to ensure the cooling of the soil-structure interface. The first step to define the thermal effects is to isolate the effect of the mechanical loading. The strain due to purely mechanical load (e.g., after 16 h), is considered to be constant, assuming that there is negligible creep effect due to load applied to the pile head over time. Accordingly, the measured strain values ($\varepsilon_{meseared}$) were zeroed by subtracting the mechanical axial strain, then, the results due to the temperature variations can be interpreted. In the final phase, and after the thermal recovery, another mechanical test was carried out exactly as the first one, up to 0.6Q_{max} (60 %), by the increments of 0.1Q_{max} (10 %) to assess the impact of thermal cycles on the bearing capacity.

The experimental program was designed to represent the energy consumption patterns in the Netherlands, which is mostly heating the building (cooling down the pile) while maintaining a constant

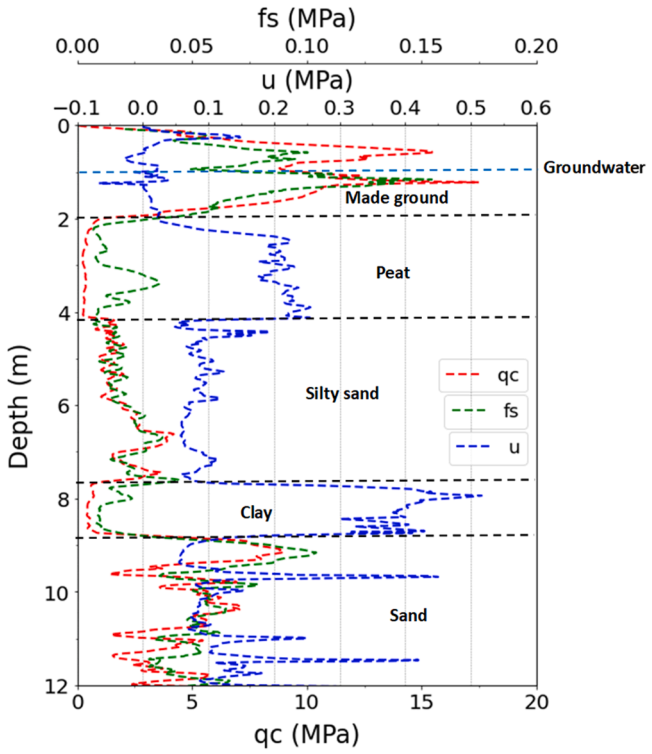

Fig. 3. The results of CPTs with soil profile: cone resistance (qc); sleeve resistance (fs); and pore water pressure (u).

Table 1
Test program.

Test No.	Type	Number of cycles	Duration of Cooling/ Natural-heating (h)	Static load (kN)
T_M1	Mechanical	-	-	0, 36, 71, 106, 141, 176, 211
T_0	Thermal	2	12/12	0
T_30	Mechanical + thermal	6	12/12	106
T_40	Mechanical + thermal	10	12/12	141
T_60	Mechanical + thermal	10	12/12	211
T_M2	Mechanical	_	_	0, 36, 71, 106, 141, 176, 211

mechanical load, mainly due to the deadweight of the supported structure.

Data processing

Thermal expansion or contraction of the energy pile can occur during heating and cooling, respectively proportionally to thermal variation. When the pile is unrestrained, the resulting (free) axial thermal strain can be expressed as follows:

$$\varepsilon_{T,\ \text{unrestrained}} = \alpha_{\text{pile}} \times \Delta T \quad (1)$$

where α_{pile} is the thermal expansion coefficient of the pile and ΔT is the temperature difference. The coefficient of thermal expansion was calculated from the results of the gauge positioned at the top (specifically, the gauge at level 1.1) during the free expansion test (T_0) when the pile had no external load and is seen to have very low shaft resistance (see Fig. 12(a)). The coefficient of thermal expansion obtained in this study, derived from the strain versus temperature variation data, was found to be −10.71 με/°C (compression positive sign convention) and this falls within the range reported in previous research where coefficients of thermal expansion for reinforced concrete in unrestrained conditions ranged from −10 to −15 με/°C.[5,7,10,22] Note that this coefficient could be slightly affected by the shaft resistance.

In energy piles, the surrounding soil provides a confining effect on the pile, constraining the possible deformations, thus, an additional axial constraint strain is generated.

For this reason, the expansion or contraction due to the applied thermal loads is generally lower than the theoretical thermal free strains. The thermal strain (ε_T) primarily hinges on the interaction between the soil and the structure.

Due to the thermal expansion of the steel wire in the temperature gauges, correction must be applied to the recorded strain readings in the following manner:

$$\varepsilon_{measured} = \varepsilon_{gauge} + \alpha_{gauge}\Delta T \quad (2)$$

where ε_{gauge} denotes the raw measurements recorded by gauges, α_{gauge} is the coefficient of linear thermal expansion of the steel wire in the gauges (11 με/°C), and ΔT is the temperature change of the gauge.

Part of the free strain is observed while another part of the pile deformation is constrained (non-manifested) by the surrounding soil, resulting in the development of internal thermal stress. The non-manifested strain is the mechanical strain (ε_m) is transformed into axial stress. It can be obtained from the thermal strain measured from each gauge by subtracting the thermal free strain. The equation used is as follows:

$$\varepsilon_m = \varepsilon_{measured} - \varepsilon_{T,unrestrained} \quad (3)$$

Accordingly, the average thermal axial stresses (σ_T) induced in the foundation by the temperature changes along the pile can be calculated as follows:

$$\sigma_T = E \times \varepsilon_m \quad (4)$$

where E denotes the defined Young's modulus of the pile, which has been calculated using the method of Fellenius[45] (41 GPa).

The pile penetrates the soil under mechanical loading and shrinks during cold load, resulting in a relative displacement between the pile and the surrounding soil, which in turn generates shear stresses along the pile shaft. The difference in axial force along the pile is caused by the shaft resistance due to the pile displacement. Hence, the mobilized shaft resistance values were determined for each load step along discrete portions of the pile (denoted by j) using the following equation:

$$\tau_j = \frac{(\sigma_{i-1} - \sigma_i)r}{2(d_i - d_{i-1})} \quad (5)$$

where σ denotes the stress calculated at different depths, r is the pile radius, d is the distance between two strain gauges, and i indicates the position of strain gauges from the top of the pile to the bottom of the pile. The sign of strain and stress values were defined such that positive denotes compression and negative denotes tension to be consistent with geotechnical sign conventions and the previous studies. While the positive and negative signs of mobilized shaft resistance values represent upward and downward friction, respectively.

Results and analysis

Mechanical behavior under multiple mechanical conditions

The mechanical results of the test T_M1 are presented in this section. The average strain gauge readings from the two strings on opposing sides of the pile were considered (see Fig. 2).

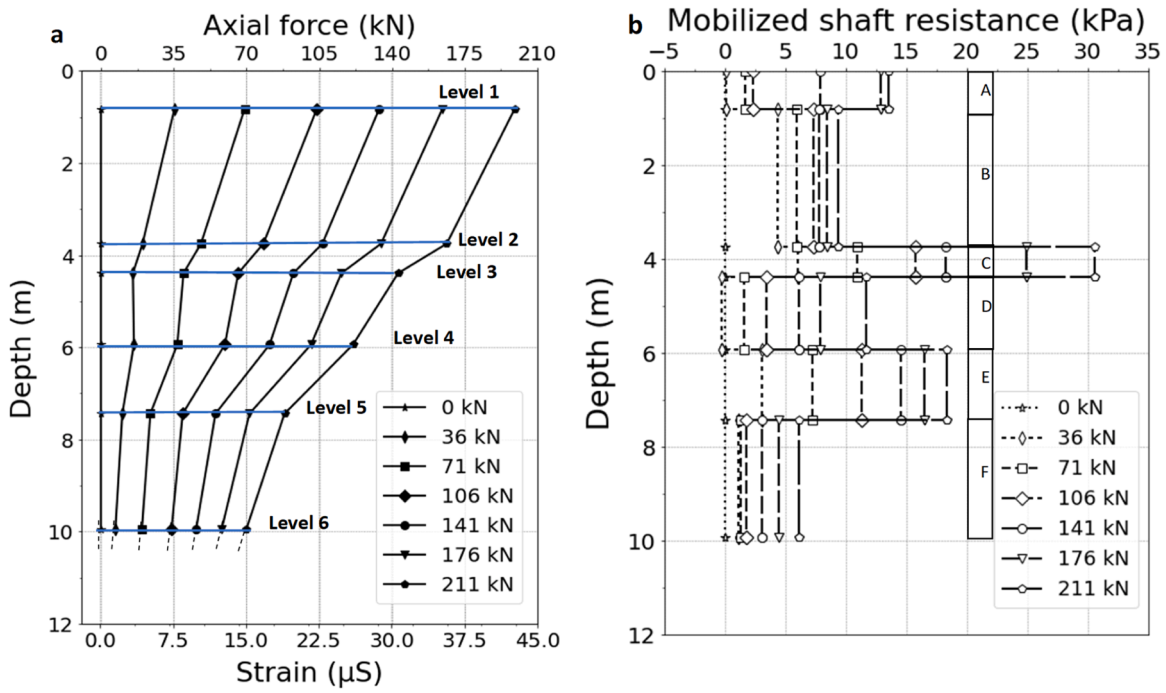

Fig. 4. Mechanical response of energy pile obtained from test T_M1 test: a) Axial strain and force at each level, b) mobilized shaft friction versus the depth at each zone.

The measured strains and axial forces along the pile in successive load steps are shown in Fig. 4(a). Any pre-existing compressive forces were not considered, i.e. strains are considered to be zero at the beginning of the load test. The application of mechanical load to the pile head tends to cause a relative displacement between the pile and the soil; therefore, the pile was affected by side friction resistance, causing a gradual decrease in the axial force and strains along the pile length. As an almost linear decrease in the force with depth can be observed, the value of the force at the pile tip, where no gauges were installed, has been estimated by extrapolation from the two last measured forces to the depth of the pile tip (i.e. 10.3 m depth). The extrapolated part is shown in dashed lines (connected to the solid lines). It should be noted that the last gauges (level 6) and the pile tip were in sandy layer and the trend of the curves is expected to be unaffected. Although the pile was installed in relatively soft and weak soil layers, approximately 70 % and 30 % of the applied mechanical load were transferred to the shaft and pile tip respectively. This distribution is likely influenced by the displacement method of installation of the pile, which densifies the surrounding soil and thus increases the shaft capacity. As a result, this pile can be considered as a "semi-floating energy pile".

Fig. 4(b) exhibits the distribution of pile mobilized shaft resistance along pile depth under different mechanical load conditions. The shaft resistance increased with increased applied mechanical load. The maximum and minimum shaft resistance were obtained at zone C (from 3.75 to 4.39 m) m and zone F (from 7.44 to 9.94 m), respectively, being 31 kPa and 7 kPa, respectively, under a load of 211 kN. The shaft resistance generally decreases with depth consistent with the reduction in applied load seen in Fig. 4(a), with increases where the soil changes to a stiffer layer. The shaft resistance in the lowest section of the pile body is the smallest, probably due to the restraining effect on the bottom of the pile body by sandy soil along with the decrease of the axial load along the pile and thus the axial displacement. However, the resistance of the whole pile body does not reach the zero value except under the lowest applied mechanical load (36 kN) at zone D (4.39–5.94 m), where −0.26 kPa was observed, this is likely due to a larger deformation of the soil in this zone than the zones above and below, and possibly a pre-existing stress at level 4.

Thermo-mechanical behavior under monotonic pile cooling

To investigate the stress variation during monotonic cooling, the results from a single cycle from all tests, where the pile temperature was reduced and kept reasonably constant, were investigated. The results of the measured temperature, the computed corresponding thermally induced stress, static loading and cooling induced stresses, and the mobilized shaft resistance at two different given moments, i.e. after 5 and 10 h, are plotted in Fig. 5(a), (b), (c), and (d), respectively. The thermal cycles and the plotted time shown are indicated in Fig. 6.

In Fig. 5(a), the temperature profiles are shown. In test T_0, nearly a 2 C° difference between the upper part (from the top of the pile to 4.39 m) and the lower part (from 4.39 to 9.99 m) of the pile is observed, due to the higher initial temperature in the upper part. In addition, a slightly larger temperature change at around level 3 (4.39 m) (i.e. see the temperature profile of the test T_0) is noted, which is likely due to the annual thermal heat evolution. While in the other tests, the difference between the upper and lower part of the pile became lower compared to the initial test 'T_0' with a lower temperature change at around level 2 (3.75 m), especially in tests T_30, which is most likely due to the low thermal conductivity of the peat (slow thermal recovery, see the temperature change at the end of test T_0); further details are discussed in the temperature variation section. In all cases, the temperature change from 5 to 10 h was reasonably constant, with the T_0 test remaining within 1°C and the other tests within less than 1°C. As observed in previous studies (e.g. Gawecka, et al. [37]), the thermally induced stresses (Fig. 5(b)) reduce with time, as the soil also contracts.

In test T_0 at Level 1, there was the lowest stress increment at all positions and for all tests due to the low pile restraint due to no surface load. Further into the soil, more significant thermal stresses were generated, reducing in time partially due to the lower temperature change and partially due to the drag-down of the soil due to its cooling further away from the pile. In the other tests (T_30, T_40 and T_60), after 5 h of cooling higher tensile stress increments were observed under higher mechanical load, especially near the pile head, while at level 3, the lowest stress was detected under the highest mechanical load, this is because of the lowest temperature change was recorded at this level in

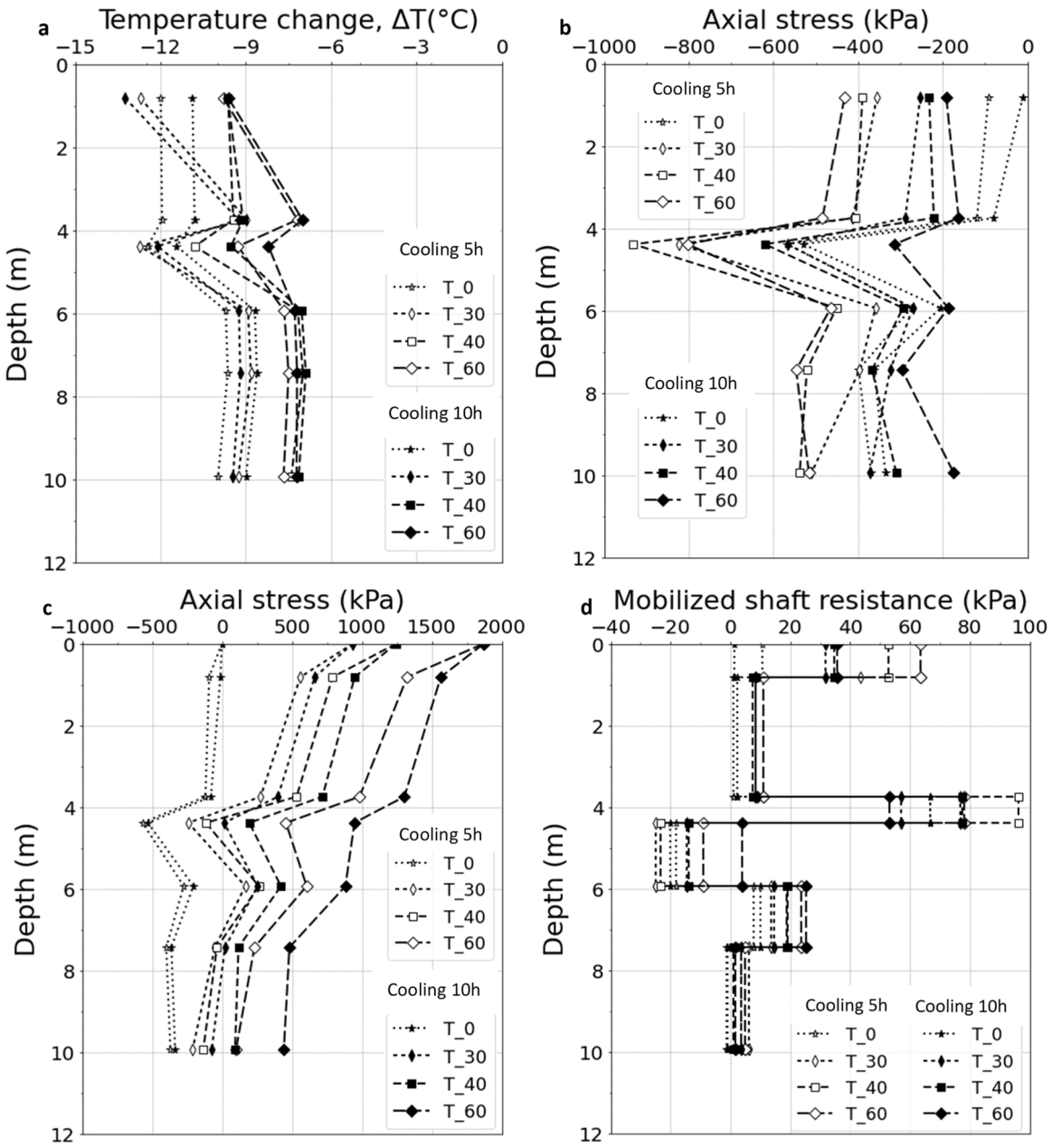

Fig. 5. Thermo-mechanical response of energy pile after 5 and 10 h of cooling obtained from the four conducted tests (T_0, T_30, T_40, and T_60): (a) Temperature variation; (b) the corresponding cooling induced axial stress; (c) corresponding static loading and cooling induced axial stresses; (d) mobilized shaft friction versus the depth at each zone.

the test T_60 (see the temperature profiles in Fig. 5.(a)). Further cooling (after 10 h) showed a significant reduction of up to 78 %, despite the constant temperature or the slight temperature variation (±1°C) in these tests.

It should be noted that the lowest tensile stress near the bottom of the pile after 10 h can be observed in the test T_60, followed by T_40, T_30 and T_0. This shift in the tensile stress can be explained by the thermal contraction of the subsurface. Moreover, the difference in the initial stress in the soil induced by the applied mechanical load may affect the magnitude of cooling-induced contraction of the soil surrounding the pile and sand beneath the pile tip leading to higher tip displacement. A higher irreversible contraction of sand was observed under higher mechanical load.[55,60] Therefore, the higher is mechanical load, the lower the tensile stress increment is.

The thermal axial stresses induced during the cold load were added to the mechanical axial stresses due to the applied mechanical load, as shown in Fig. 5(c). The thermo-mechanical axial compressive stresses in the test T_60 are 1.55 MPa and 0.5 MPa near the top and the bottom of the pile respectively, after 10 h of cooling. The observed magnitudes of the axial stresses are all much less than the compressive strength of concrete (estimated at 22 MPa). Note that the cooling load reduces the net compressive stresses that were initially induced due to the applied mechanical load. A similar observation was reported by Jiang et al. [59]

Fig. 5(d) represents the mobilized shaft resistance profile of the energy pile of the test T_0, T_30, T_40, and T_60, which was determined based on the axial stresses of the pile. In the test (T_0), the pile shaft friction resistance was significantly lower than those under the combined effect of static loading and cooling (T_30, T_40, T_60) as seen in Fig. 5(d). Additionally, the mobilized shaft resistance decreased with further cooling of the pile (from 5 h to 10 h) in the four tests. As the axial stresses are seen to reduce after ten hours of cooling, so does the mobilized shaft resistance. In the free expansion test (T_0), after 10 h of

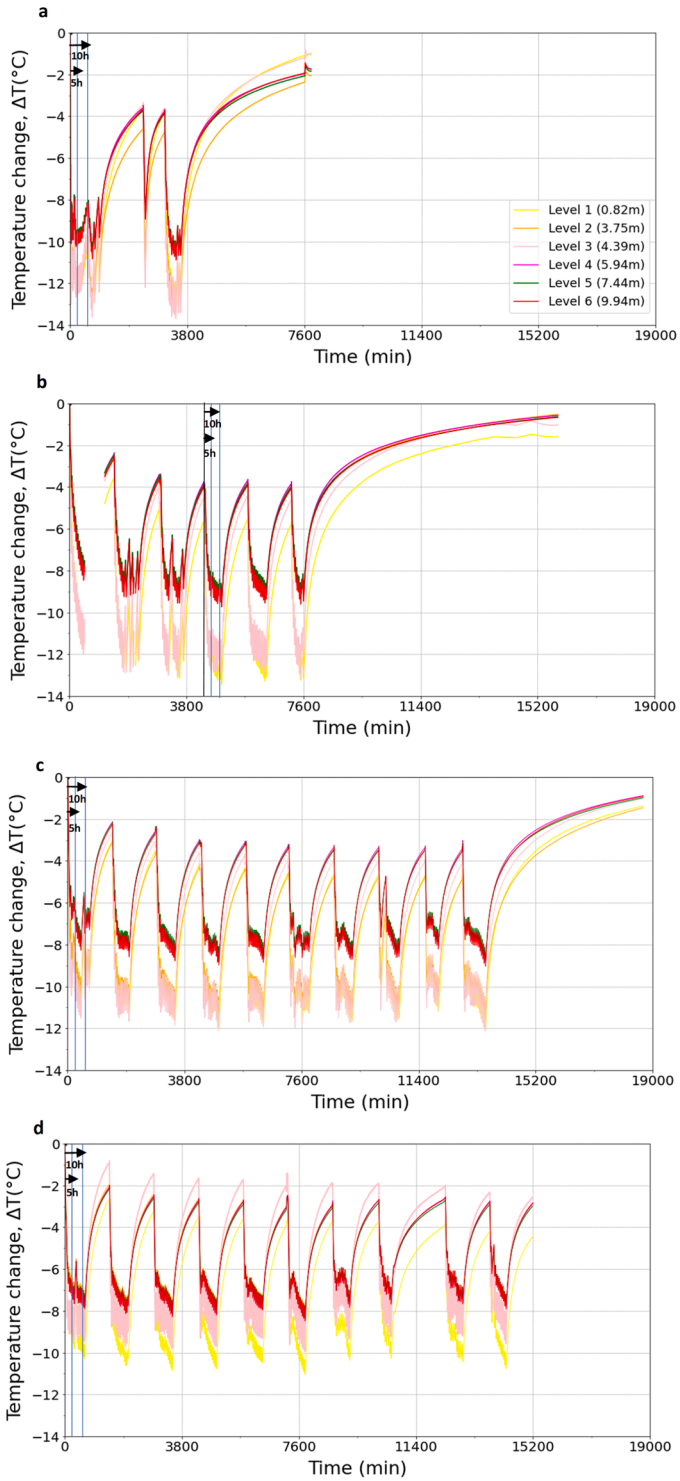

Fig. 6. Measured temperature change along the energy pile in the test with two different given moments, i.e. after 5 and 10 h of cooling: (a) T_0, (b) T_30 (*level 3 is hidden by level 4*), (c) T_40, (d) T_60.

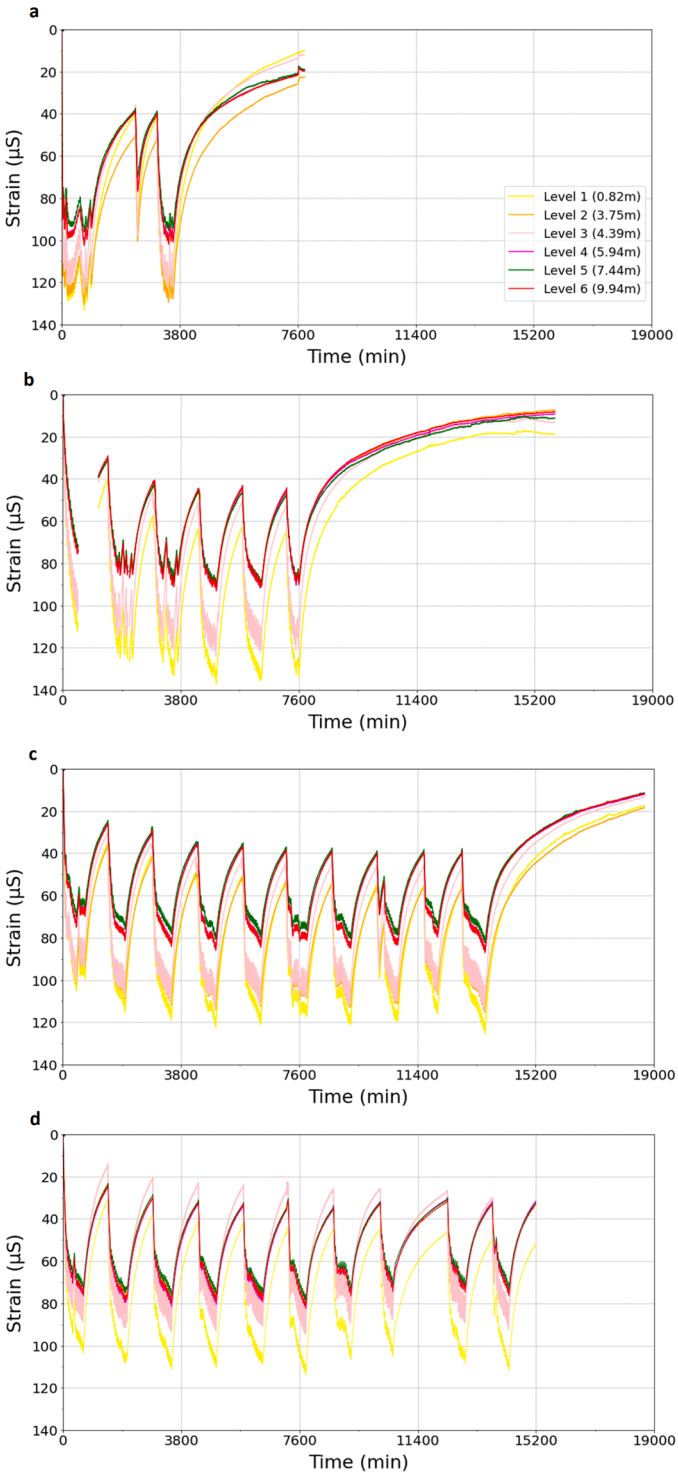

Fig. 7. Thermally induced strain increments variation of the pile versus elapsed time during thermal cycles of the test: (a) T_0, (b) T_30, (c) T_40, (d) T_60.

cooling, 1 kPa and −1 kPa of mobilized shaft resistance were observed near the top and the tip of the pile respectively, demonstrating, that the generated positive and negative side friction resistance, respectively reflects the upward and downward constraints of the soil under the downward and upward contraction of the pile during cooling from the pile head and bottom respectively. In test T_60, 35 kPa was obtained near the top which was higher than observed due to purely mechanical load (12 kPa under the same mechanical load condition), and 1.5 kPa near the pile tip which was lower than observed in the test T_M1 (7 kPa under the same mechanical load condition) by the reason of the pile shrinkage from both ends of the pile, the mobilized shaft resistance increased at the top and decreased at the bottom after applying cold load. It should be noted that negative friction was detected at zone D, likely due to the larger decrement in axial stress as a result of a larger decrement in temperature variation and maybe a larger contraction of the soil near this zone compared to the pile.

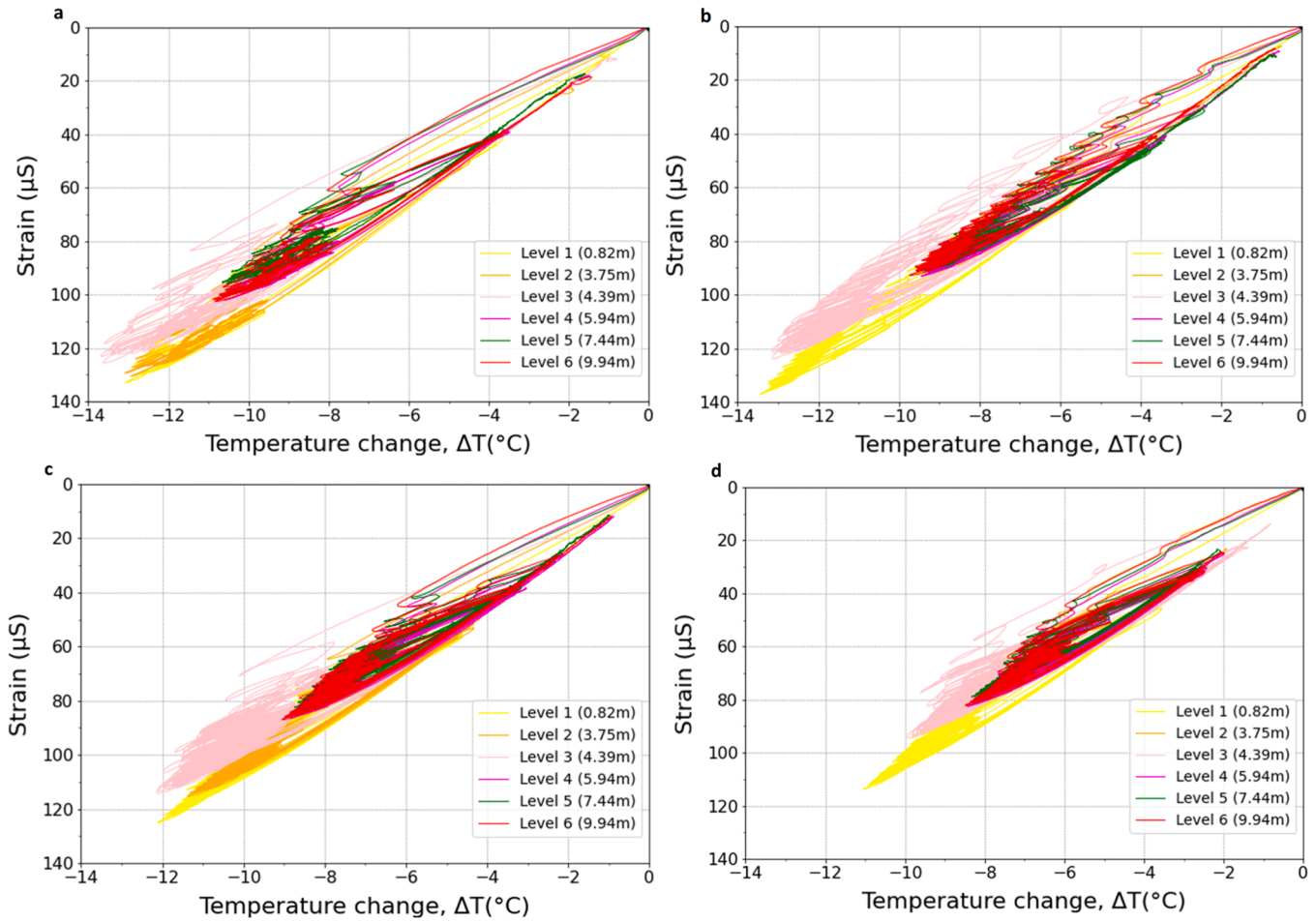

Fig. 8. Thermally induced strain increments variation of the pile versus temperature change during thermal cycles of the test: (a) T_0, (b) T_30, (c) T_40, (d) T_60.

Thermo-mechanical behavior under thermal cycles

Temperature variations

Fig. 6 shows the temperature variation versus elapsed time for the tests T_0 (Fig. 6(a)), T_30 (Fig. 6(b)), T_40 (Fig. 6(c)), and T_60 (Fig. 6 (d)). The highest temperature variation was observed in the test T_0 followed by T_30, T_40 and T_60, the decrement in its magnitude can be attributed to the residual reduction in energy gradually accumulated in the soil surrounding the pile after each thermal test, noting that the minimum temperature of all the conducted tests was above the freezing point (0 °C) along the pile (the initial ground temperature below 4 m was 12 °C). Note that within the cooling phase, the variability can be seen due to the stoppage time of the GSHP. In each test of the conducted thermo-mechanical tests, the cooling target was nearly similar throughout the test while during natural heating in the first 3 thermal cycles, the temperature was not fully recovered and tended to decrease due to the reduction in thermal energy in the soil surrounding the pile. In the following cycles, the magnitude of temperature variation stabilized. The average temperature reduction at the end of the thermal cycles in the conducted tests T_0, T_30, and T_40 was approximately −1.5 °C, while in the test T_60 it was −3 °C. The measurements of the temperature variation demonstrate that the temperature distribution along pile depth was non-uniform. In the first test T_0, during the first cooling phase, the highest pile temperature variation was detected at the upper part of the pile from 0 to 4.39 m (i.e. at the first 3 levels) and it decreased in the lower part from 4.39 m to bottom (i.e. at the last 3 levels). It should be noted that a higher residual low-temperature change at level 2 can be observed due to the low thermal conductivity of the peat. In the subsequent tests, the temperature variation is dependent on the initial conditions (see the temperature change at the end of each test). As stated in the monotonic results, test T_30 displayed a prominent decrement in temperature variation at level 2 (lower than levels 1 and 3), attributed to the peats' slow thermal recovery (see the temperature change at the end of test T_0). Similarly, in the last test (T_60), there was a significant decrease in temperature variation in the upper part. This follows from observations in test T_40, where a large temperature change at this level resulted in a higher residual temperature variation at the end of this test.

Thermally induced strain

The (incremental) axial strains $(\varepsilon_{measured})$ are shown in Fig. 7(a), (b), (c), and (d) for the tests T_0, T_30, T_40, and T_60, respectively. As expected, contraction was observed during cooling, and during natural heating expansion reduced the net contraction. The thermal axial strain was observed to vary with depth in the foundation, and generally reduces, due to the restraint provided by the soils along the pile. In the upper part of the pile (levels 1, 2, and 3), the thermal strain results of the first test T_0 demonstrated that the highest contraction occurred near the top, at level 1, followed by level 2, with the lowest observed at level 3. Interestingly, the highest temperature variation was measured at level 3 (Fig. 7). This discrepancy can be attributed to the impact of boundary conditions and the varying degrees of restraint provided by the stiffness of the surrounding soils. Different restraint conditions induce different magnitudes of strains. In the upper part, the weakest restraint conditions are imposed by the made ground and peat (levels 1 and 2) contrast with the stronger restraint imposed by silty fine sand (level 3), where higher stress levels are expected (see Fig. 9). In the lower part (levels 4, 5, and 6) the results showed the lowest strain was at level 5 followed by 4 and 6, despite level 6 being located in a sand layer, which was expected to

Table 2
Residual strains.

Test	Level	$R_{T,\ unrestrained}$%	R_{obs} %	ΔR%
T0	Level 1	8	8	0
	Level 6	16	18	2
T30	Level 1	13	14	1
	Level 6	7	9	2
T40	Level 1	12	14	2
	Level 6	10	13	3
T60	Level 1	44	47	3
	Level 6	36	43	7

exhibit the highest stiffness (Fig. 7). This may be due to the densification of the surrounding soil during the installation of the pile, which might have increased the shaft resistance across all soil layers, leading to nearly similar restraint conditions. Moreover, the thermal strains in the energy pile are likely governed by the average temperature of the pile and the surrounding soil rather than the local temperature measured at the strain gauge locations.[11,47,48] With the increase in the number of temperature cycles during thermo-mechanical tests, the thermal strain curves manifested a downward trend, leading to a residual strain at the end of these tests. The axial strain behavior can be better evaluated by investigating the trends in thermal axial strain plotted against temperature change measured at each gauge depth, as shown in Fig. 8(a), (b), (c), and (d) for T_0, T_30, T_40, and T_60, respectively.

Across all gauges, the curves show some degree of hysteresis, with the lowest amount being observed in the free expansion test (T_0) at all levels. This indicates a potential ratcheting effect under thermo-mechanical loads, which appear to be dependent on the applied mechanical load.[57] The higher the mechanical load, the higher the amount of hysteresis is. This phenomenon can be attributed to the stoppage/start operation of GSHP within cooling load (noted previously as variability in temperature) leading to decrease/increase of thermally induced strain and also the incomplete pile and soil temperature recovery during natural heating, resulting in an increase in low-residual temperature over cycles in each test (see Fig. 6). The studies on soil-structure interfaces by Golchin et al.[33] and Rafai et al.[34] showed a shear displacement due to the thermal load in a ratcheting pattern. This may explain the potential ratcheting. Another plausible explanation involves the gradual cooling of the sand beneath the pile over time within a load level test, causing shrinkage in the sandy soil, which was allowed to recover before the next load level test.

Although the pile was subjected to different mechanical load conditions and temperature magnitudes, the thermal axial strains appear to be dependent on the applied mechanical load and are likely governed by temperature variations. Additionally, the thermo-elastic contraction and expansion of the energy pile was slightly affected by the load level. Nevertheless, residual thermal strains can be observed at the end of all conducted tests, with higher strains observed under higher mechanical loads. This finding aligns with similar observations reported in previous studies.[16,18]

To separate the effects of low-residual temperature in the pile from those induced by the ground, (potentially its permanent deformation), changes in axial free strain ($\Delta\varepsilon_{T,\text{unrestrained}}$) (calculated from temperature data using Eq. (1)), and measured axial thermal strain ($\Delta\varepsilon_T$) at the end of each test, were normalized with respect to the upper bound of axial thermal free strain ($\Delta\varepsilon_{T,\text{unrestrained,max}}$) and the measured axial thermal strain ($\Delta\varepsilon_{T,\text{max}}$), which represent the residual axial free strain ($R_{T,\text{unrestrained}}$%) and residual axial thermal strain (R_{obs}%) respectively. The difference between these residuals indicates the permanent residual thermal strain due to the drag-down of the surrounding soil (ΔR%). These results are shown in Table 2 for levels 1 and 6, near the pile head and tip, respectively.

The permanent residual thermal strains (ΔR%) close to the pile tip (level 6) are higher than those observed close to the pile head (level 1) in the four conducted tests. Additionally, this permanent residual thermal

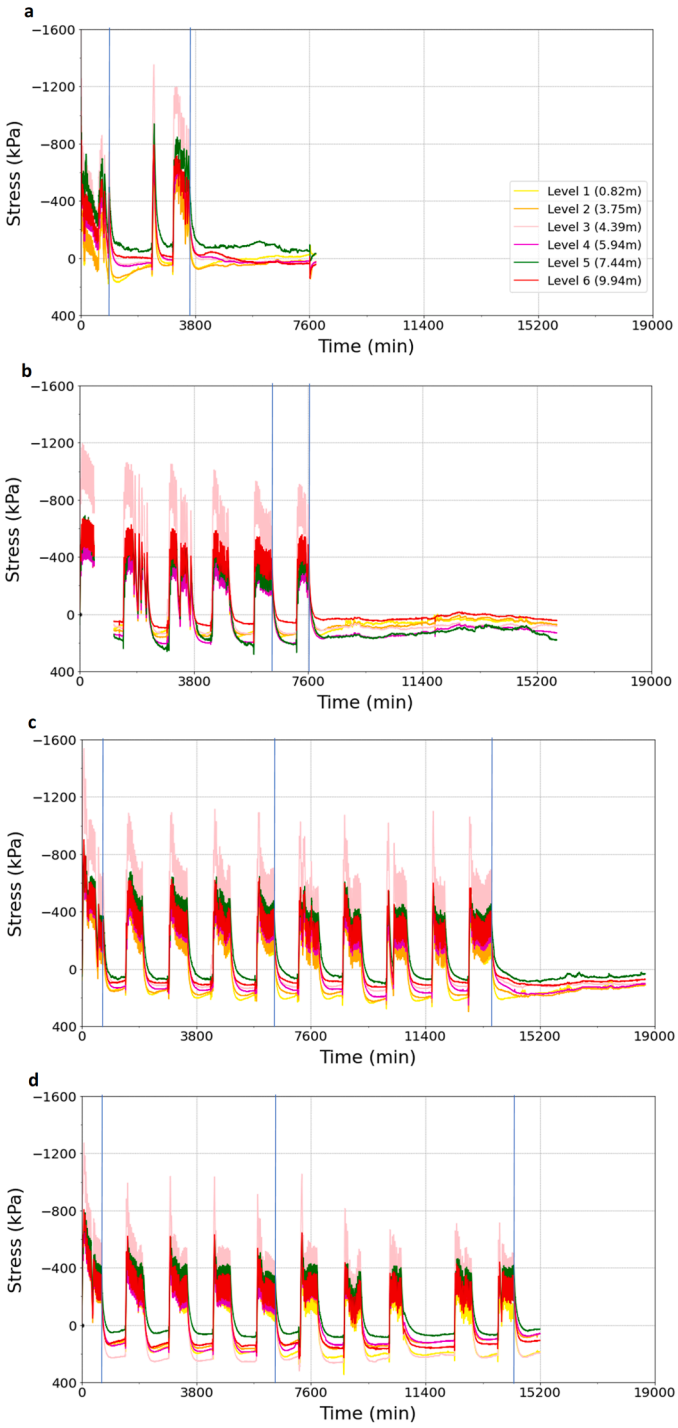

Fig. 9. Thermally induced stress increments variation of the pile versus elapsed time during thermal cycles of the test: (a) T_0, (b) T_30, (c) T_40, (d) T_60.

strain increases with increasing mechanical loads at both levels. These results implied that the thermal contraction of the surrounding soil, including the sand beneath the pile tip during thermal cycles, depends on the applied mechanical load. This phenomenon could impose a drag-down effect on the pile shaft, inducing residual contractive strains within the pile, particularly under higher mechanical loads. Moreover, the permanent contraction of sand could induce residual thermal strain at the end of the thermo-mechanical tests, along with potential mechanical creep. In the free expansion test (T_0), the thermal strain at level 1 appears to be perfectly thermo-elastic. However, at level 6, a residual plastic deformation can be observed due to the successive drag-

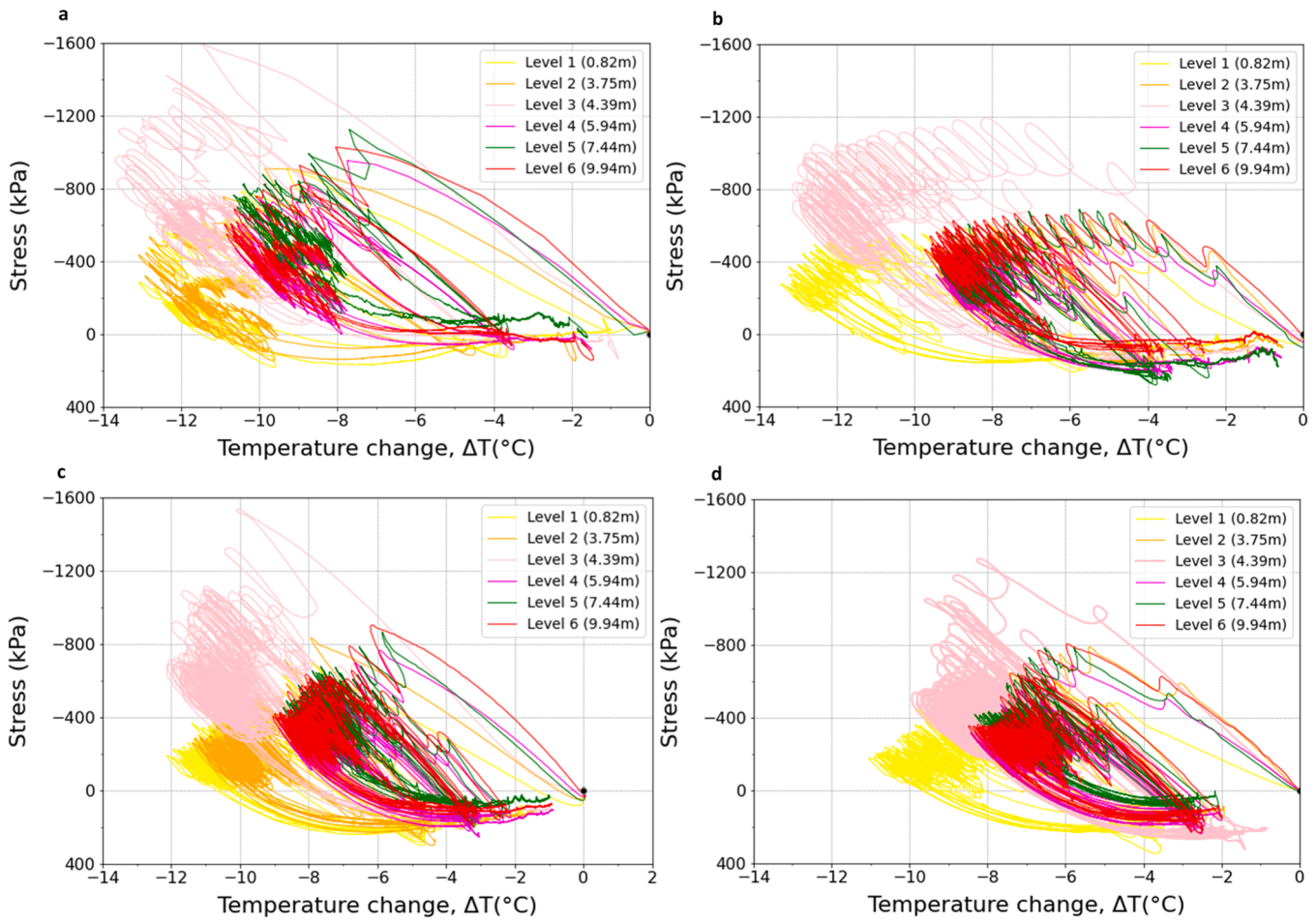

Fig. 10. Thermally induced stress increments variation of the pile versus temperature change during thermal cycles of the test: (a) T_0, (b) T_30, (c) T_40, (d) T_60.

down of the surrounding soil layers, inducing higher force at the lower part of the pile. This restricts the potential expansion of the pile (i.e. the total reduction of the net contraction) during natural heating. Similar observations are noted in the other tests, where the successive settlement of the subsurface tends to induce higher force at the pile tip, leading to higher plastic residual strain in the four tests compared to level 1 (Figs. 7 and 8).

Thermally induced stress

The results of thermally induced stresses during thermal cyclic loading in all tests versus elapsed time are shown in Fig. 9(a), (b), (c), and (d) for the energy foundation under 0 %, 30 %, 40 %, and 60 % of the estimated bearing capacity, respectively. These results reflect the changes in axial stress within the pile due to the applied thermal load. It can be observed that cooling decreased the axial stress at all levels, indicating a tensile stress increment, and the latter increased during natural heating, resulting in a compressive stress increment.

During the free expansion test (T_0), when the pile had the greatest freedom to deform, the lowest tensile stress was generated during cooling. This stress was nearly fully recoverable, especially at level 1 with minor residual stress at the other levels. However, when the pile was restrained by the applied mechanical loads (T_30, T_40, and T_60), the tensile stress increment was relatively higher under higher mechanical load during cooling (with respect to the temperature change), and subsequent natural heating led to a notable compressive stress along the pile shaft in all tests. When the cooling phase started (before transferring the cold load to the subsurface), maximum tensile stress was generated, which decreased over time during the cooling phase. This decrement was higher under higher mechanical load, as shown by monotonic results. Similarly, the maximum compressive stress was generated during natural heating. It can be observed that the tensile stress increments decreased with increasing the number of cycles. The stress change in the pile during cooling and natural heating cycles may include residual compressive stresses and thermally induced stresses, leading to a residual contractive stress at the end of these tests (i.e. a shift from tensile to contractive stress). The development of residual compressive stresses at the end of each cooling-natural heating cycle led to lower tensile stresses and higher compressive stresses during pile cooling and natural heating, respectively. This phenomenon can be explained by the combined effects of the drag-down of the surrounding soil due to the subsurface shrinkage during the cold load and the compression imposed on the pile head. Another possible explanation is related to the mechanical and thermal creep effects; when the pile was under pure mechanical load, the period before the thermal load was dependent on the applied load. Consequently, the period when the pile was under a lower mechanical load was shorter, affecting the magnitude of the creep effect. As stated previously, the thermal creep at the pile interface as well as the drag-down of the surrounding soil could alleviate the tensile stress.

Stress variation of the pile versus temperature change during thermal cycles of the four tests, T_0, T_30, T_40, and T_60 are shown in Fig. 10(a), (b), (c) and (d) respectively. It can be noted that hysteresis was lower under zero mechanical load. However, once an applied load was introduced, an important amount of hysteresis can be observed (similar to the strain results), probably due to the ratcheting effect combined with the drag-down of the subsurface. Thermally induced stress evolution at the end of cooling load at different cycles (see the blue lines on Fig. 9(a), (b), (c), and (d) where the measurements were taken) versus depth is shown

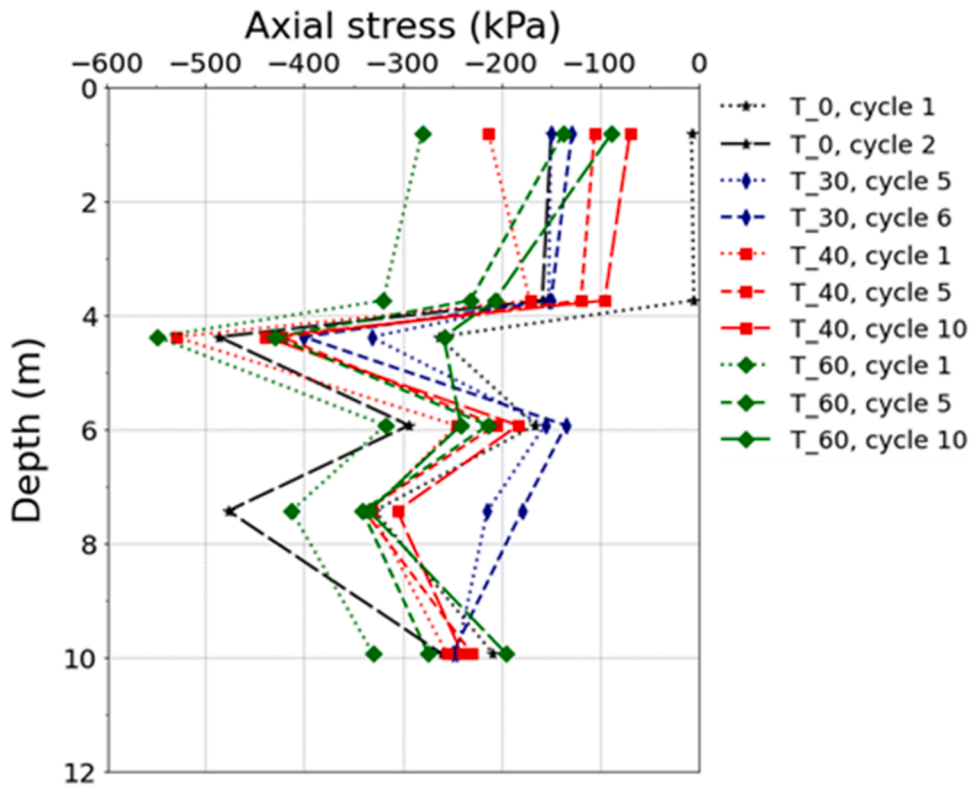

Fig. 11. Thermally induced stress evolution versus depth.

in Fig. 11. This figure shows a decrease in the axial stress with increasing number of thermal cycles (e.g. see T_60, cycle 1; T_60, cycle 5; and T_60, cycle 10).

It can be seen that the stress (at the first cycle, before its reduction) near the pile head strongly depends on the applied mechanical load and it is higher under higher applied mechanical load, although the temperature was lower (similar to monotonic cooling results). However, further with depth, at other levels, the axial stress seems to be dominated and impacted by the temperature variation and slightly by the mechanical load. This is because the load was away from these levels compared to level 1 (where the load was immediately above this zone), indicating that at such zones shaft resistance plays a significant role in the thermally induced stresses.

It should be noted that the soil at the surface was free to deform, and the normal stress tends to increase with the depth. Consequently, interparticle shear force at the interface may also increase with the depth, enhancing the tendency of the soil grains to slip and rearrange in response to additional loading. When these grains were subjected to cold load, their diameter shrinks, causing a decrement in the overall volume. In addition, their contraction and expansion during cooling and natural heating cycles would be more pronounced, as they are more susceptible to thermally induced perturbation. This results in slippage and rearrangements, and therefore, more plastic deformation at the bottom compared to the top, where the normal stress is minor, further details are provided by Rafai et al. [60] This can explain the residual thermal strain observed previously in the test T_0 near the pile tip. Furthermore, imposing additional mechanical loads induces stress at the soil-structure interface and the pile tip which may render the nearby soil more susceptible to irreversible thermally induced contraction due to simultaneous contraction, expansion and rearrangements of grains under thermo-mechanical loads. Consequently, subsurface shrinkage is higher under higher mechanical load. The successive settlement of the surrounding soil might reduce (even temporarily or partially "in some zones") the pressure at the soil-structure interface, leading to higher permanent contractive strain (see Fig. 7) and lower tensile stress (see Fig. 9) during cooling, compounded by potential mechanical creep effects. Furthermore, the repeated contraction and expansion cycles may exacerbate the soil-structure interface load redistribution due to the grains' rearrangement. In such cases, the load would shift from the shaft to the tip to compensate for this degradation, leading to a denser sandy soil beneath the pile and therefore higher tip resistance.

McCartney and Murphy[11] reported approximately −0.7 MPa thermally induced stress increments in an end-bearing energy pile embedded in claystone, with an average temperature variation of −3.3 °C. Kong et al.[18] reported approximately −1 MPa for a belled energy pile embedded in sandstone, with an average temperature variation of −8 °C during the first cooling cycle. In this study, −0.51 MPa with an average temperature variation of −7.6 °*C* was observed, specifically, in test T_60 after 5 h of cooling.

It is seen that within the same energy pile (see Fig. 11) non-uniform stresses were induced along the pile, depending on the restraining effect by the surrounding soils, and temperature change. This aligns with the numerical analyses performed by Abdelaziz and Ozudogru.[48] Therefore, quantitative differences are expected when comparing the obtained results in this study with other studies in different conditions.

All these piles were restrained at the top by either a building or an applied load, with the axial stress near the pile bottom depending on pile restraint from the soil. This restraint condition at the bottom of the pile can be quantified by the degree of freedom n, where a low value of n indicates a high restraint:[46]

$$\mathrm{n} = \frac{\Delta\varepsilon_T}{\Delta\varepsilon_{T,\mathrm{unrestrained}}}$$

Here, $\Delta\varepsilon_{T,\mathrm{unrestrained}}$ and $\Delta\varepsilon_T$ are the changes in the unrestrained thermal strain and observed thermal strain, respectively.

In this study, the degree of freedom near the bottom of the energy pile in test T_60, was 0.77 after 5 h cooling. In contrast, the end-bearing pile studied by McCartney and Murphy[11] was 0.47, and the belled pile by Kong et al.[18] was 0.32. For this reason, the highest axial tensile stress was observed in piles with the highest restrained at the tip, indicating

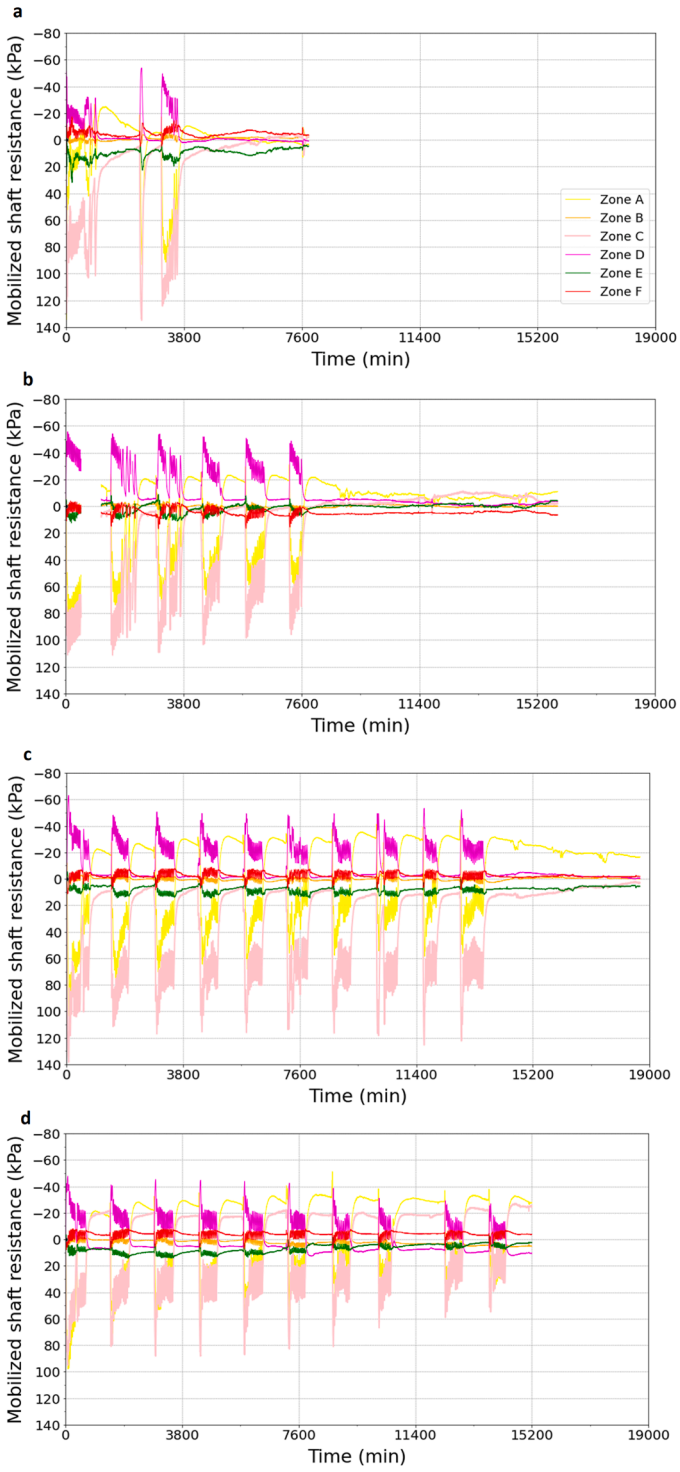

Fig. 12. Mobilized shaft resistance variation of the pile versus elapsed time during thermal cycles of the test: (a) T_0, (b) T_30, (c) T_40, (d) T_60.

the lowest degree of freedom. In cases where energy piles are embedded in stiff soil (such as those studied by McCartney and Murphy[11]) both radial and axial thermal expansion/contraction are restrained by the high stiffness of the soil, resulting in higher thermally induced stress. However, in this study, where the pile was embedded in soft (expansive/contractive) soil, the initial stress at the first moment of thermal load (i.e. during cooling) was lower compared to the stiff-soil scenario of the studies by McCartney and Murphy[11] and Kong et al.[18] In addition, when the cold load was transferred to the surrounding soil, this caused shrinkage, thereby reducing tensile stress. This process facilitated the transfer of stress to the ground. It is evident that thermally induced stresses are likely to be higher when the piles are in stiff soils, especially in the case of end-bearing piles. This may contrast with floating and semi-floating energy piles in soft soils highlighting a critical consideration that should be factored into the design of end-bearing energy piles.

Overall, the thermo-mechanical tests indicated that only under zero axial load, a perfectly thermo-elastic behavior could be noted (Fig. 7), especially near the pile head. Once the mechanical load began to be applied at the pile head, the drag-down effects began to appear. The residual contractive strains and stresses observed along the pile can be then attributed to the irreversible strain of soil surrounding the pile toe and of the pile-soil interface, which is manifested clearly as a reduction in the tensile stress. The behavior of the pile and the effects of temperature cycles on its mechanical behavior are likely governed by the thermal elasticity of the pile and thermo-hydro-mechanical coupling in the surrounding soil. The overlap of the thermally induced tensile stress with the compressive stress induced by drag-down led to an insignificant effect on the energy pile. This may not hold true for larger diameter piles, where the complete shrinkage of the surrounding soil would require a longer time to occur.

Mobilized shaft resistance during thermal cycles

The shaft friction resistance was calculated from the stresses shown in Fig. 9 and obtained from two adjacent layers of strain gauges. The variations in mobilized shaft resistance for each zone (as delineated in Fig. 4(b)) along the pile versus elapsed time during thermal cycles of the four tests, T_0, T_30, T_40, and T_60 are shown in Fig. 12(a), (b), (c) and (d) respectively, while their variations with temperature change are shown in Fig. 13(a), (b), (c) and (d) respectively.

In zone A, near the pile head, observations from Fig. 12 and Fig. 13 suggest that at the initial cooling phase, the mobilized shaft friction appeared to be higher under higher mechanical load. Subsequent cooling led to a drastic decrement in the upward friction, especially under higher mechanical load. For example, in test T_30 the initial shear stress that was generated at the first moments of cooling was about 80 kPa while in test T_60 was about 95 kPa. Moreover, during the sixth cooling cycle, the shear stresses were approximately 45 and 40 kPa in tests T_30 and T_60 respectively. Similarly, natural heating induced higher downward friction under higher mechanical load. Additionally, in this zone, the results revealed an upward trend due to the decrement of positive friction and increment of negative friction accumulated after each thermal cycle, leading to a residual negative friction, which is more pronounced under higher mechanical load. Note that at the end of the free expansion test, almost no shear stress was observed, indicating full recoverability. A similar trend can be seen in zone C of these tests, while the opposite was observed in zone D.

In zone F, clear negative friction can be observed only in the free expansion test T_0. Additionally, residual negative shear stress was noted at the end of this test (T_0), due to the successive drag-down of the near soils. This is in alignment with the residual compressive strain previously. However, when the pile was under mechanical load, initially, positive friction was evident, possibly due to a larger settlement along the pile. In certain cycles under higher mechanical loads, a switch from positive to negative friction was observed, due to the pile's additional shrinkage coinciding with soil contraction as a result of the cold load. It should be noted that higher positive friction was observed in zone C compared to zone A, while the strain results revealed the opposite (higher contraction at level 1 compared to level 3) due to the higher resistance imposed by the silty sand layer compared to the made ground layer. In the four conducted tests, the lowest shear stress (nearly zero) was observed at zone B; maybe due to the low resistance combined with soil deformation.

In thermo-mechanical tests results, the shear stress appears to be higher under lower mechanical loads in zones C and D. This is possibly because of the higher contraction/expansion magnitude during cooling/

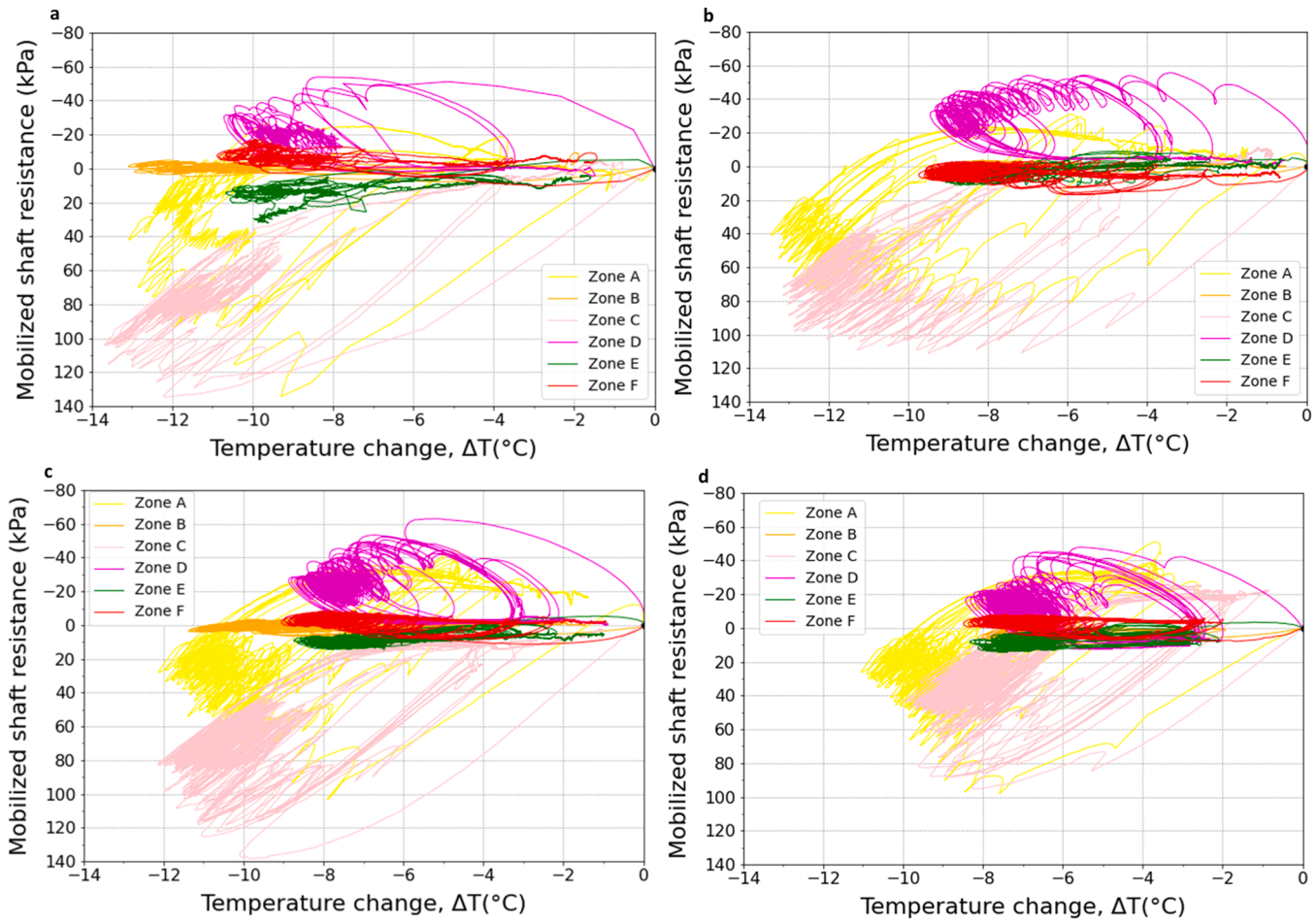

Fig. 13. Mobilized shaft resistance variation of the pile versus temperature change during thermal cycles of the test: (a) T_0, (b) T_30, (c) T_40, (d) T_60.

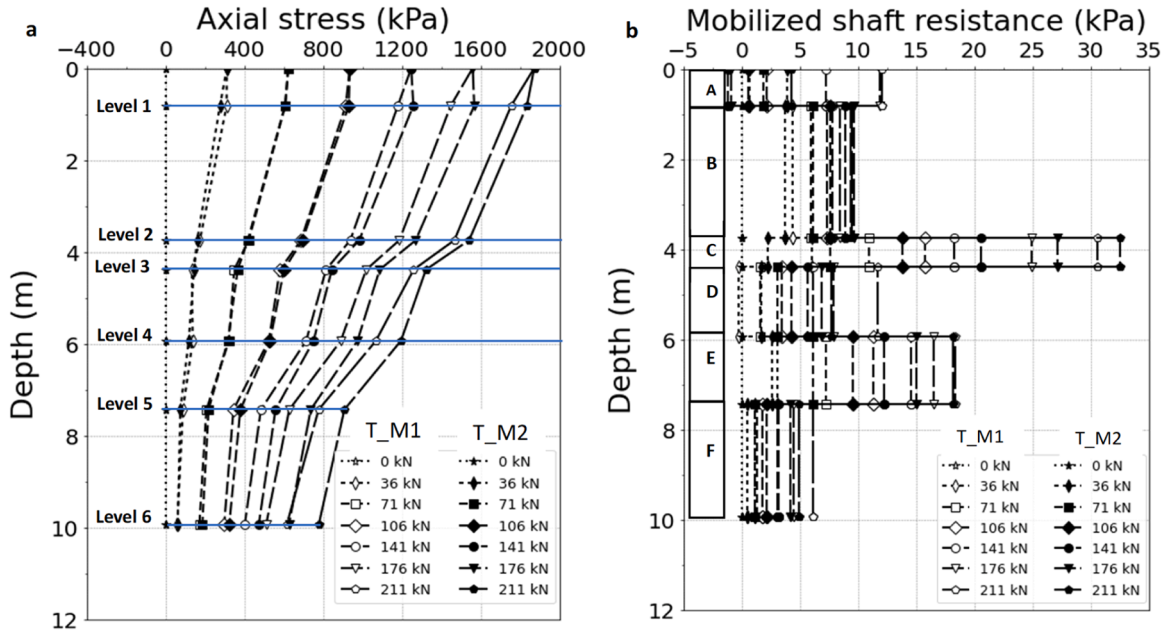

Fig. 14. Mechanical results of the tests T_M1 and T_M2: (a) Axial stress and (b) Distributions of side friction resistance along pile depth under different mechanical conditions.

natural-heating under lower mechanical load compared to higher mechanical loads due to higher temperature change and low-restraining effects. As explained previously, the impact of the applied mechanical load reduces with depth. At the end of these tests, residual shear stresses were observed at almost all zones, being higher under higher mechanical loads, due to the thermal creep at the pile-soil interface and the drag-down of the subsurface,[60,61] these were manifested as hysteresis during thermal cycles and stress reductions within cooling load as well as over multiple thermal cycles.

Thermo-mechanical creep, varying degrees of shrinkage at the soil-structure interface, and the sand beneath the pile tip could induce different magnitudes of strains, stresses, and therefore mobilized shaft friction. When the energy pile was subjected to a higher mechanical load (e.g. 60 %), additional downward strains due to the drag-down process would lead to a more nonlinear response during cooling and natural heating phases. While this effect was insignificant in a semi-floating energy pile, it should be considered in floating energy piles installed in very soft soil layers that could experience drag-down and ratcheting.

The impact of thermal cycles on the pile shaft capacity

Fig. 14(a) displays the axial compressive stress due to the applied mechanical loads, during both T_M1 and T_M2 mechanical tests, with Fig. 14(b) presenting the shear stress profiles during these tests. In both tests, under the same level of static load, the axial and shear stresses along the pile length decreased. The pile stresses of the two mechanical tests under lower mechanical load, 36–106 kN are nearly identical. However, under higher loads, the axial compressive stress increased in the last mechanical test (after the testing program), indicating lower shaft resistance. This lower resistance is observed as different shear stress in zone A and in zone D, between test T_M1 and T_M2 (see the slopes from pile top to level 1 and from level 3 to level 4, of the two tests in Fig. 14(a)), while in the other zones, the slopes appear to be almost the same, and even increases in zone C, implying a minor impact on shaft resistance per length, with differences shown in the mobilized shaft resistance in Fig. 14(b). It should be noted that the observed difference in the axial stresses, especially near the pile tip in the two mechanical tests could be due to the slight decrease in shaft resistance and also the thermally induced residual mechanical strains after thermal recovery, as seen in Table 2. The results of thermal test (T_0) imply an elastic behavior with small plasticity near the pile tip, while significant plasticity due to the drag-down was observed in the thermo-mechanical tests and thus the observed impact on shaft resistance is most likely related to the combined effects of thermo-mechanical loads.

Cyclic shear strain or thermal creep due to the contraction and expansion (horizontal and vertical) along with the soil drag-down could affect the pile-soil interface, particularly ground made layer which is initially weak and lead to a reduction of the pressure at the pile-soil interface. Such conditions could lead to soil softening, thereby decreasing the restraint on the energy pile and leading to greater contraction during the final mechanical load test and a rapid transfer of the applied mechanical load to level 1. This may explain the higher decrease of the shear stress under higher mechanical loads in the affected zones (A and D), while the thermally induced pile-soil interface settlement is expected to be higher under higher mechanical loads.[27]

Although the pile had been subjected to several stress histories, the shaft resistance remains relatively unaffected (apart from zones A and D), likely because of the ground densification during the pile installations. This phenomenon is in line with observations by Ren et al.[17], Liu et al.[29] and Kong et al.[49] This shaft shear stress reduction was observed in laboratory studies, reported, for example, by Golchin et al.[33], Rafai et al.[34], Guo et al.[58] and Rafai et al.[60].

Conclusions

A set of experiments was conducted to investigate the coupling effect of mechanical loads and thermal cycles on the mechanical behavior of a displacement energy pile under different mechanical loads (0 %, 30 %, 40 %, 60 % of calculated bearing capacity) and subjected to up to ten cooling-natural heating representing a geothermal installation working in winter mode (heating the building and cooling the foundation).

The following conclusions can be drawn:

- Under the sole influence of thermal cycles, the energy pile exhibited elastic behavior, showcasing a fully reversible pile strain and stress, especially near the pile head.
- Introduction of mechanical loads resulted in the observation of thermally induced residual irreversible compressive strain and stress along the pile. Notably, higher residual values were observed near the pile tip compared to the pile head, potentially due to ground shrinkage effects.
- Tensile stress exhibited a decreasing trend with an increasing number of cycles, due to drag-down effects on the nearby soil, leading to residual contractive stress. Moreover, higher mechanical loads correlated with higher initial tensile stress, especially near the pile head. Furthermore, the dominated impact of the applied mechanical load reduces with depth and becomes mostly driven by the shaft resistance and the temperature magnitude.
- This study indicates that strains and stresses caused by cyclic thermal loading are within acceptable limits for typical engineering structures. Axial internal stresses within the pile did not exceed its strength limits and even reduced the initial stress due to the applied mechanical loads.
- While a reduction in shaft resistance was observed, its extent was limited to only two zones, while the other four zones remained unaffected. This reduction was mainly attributed to pressure reduction as a result of the drag-down of the surrounding soil and thermal creep along the pile-soil interface due to the combined effects of thermo-mechanical loads.
- Displacement cast in-situ energy piles, in contrast to other types of energy piles, show only a minor reduction in shaft resistance when subjected to multiple thermal cycles. Their use allows continued high load transfer to the shaft and only a minor impact of long-term thermo-mechanical loads on the shaft capacity.

CRediT authorship contribution statement

Mouadh Rafai: Writing – review & editing, Writing – original draft, Visualization, Validation, Resources, Methodology, Investigation, Funding acquisition, Formal analysis, Data curation, Conceptualization. **Diana Salciarini:** Writing – review & editing, Validation, Supervision, Resources, Project administration, Funding acquisition, Formal analysis. **Philip J. Vardon:** Writing – review & editing, Validation, Supervision, Resources, Project administration, Funding acquisition, Formal analysis.

Declaration of Competing Interest

The authors declare that they have no known competing financial interests or personal relationships that could have appeared to influence the work reported in this paper.

Acknowledgements

Part of the work presented was carried out within the scope of the following projects: Netherlands Organisation for Scientific Research (NWO) project number 14698 “Energy Piles in the Netherlands”; COST Action CA21156 “European network for FOstering Large-scale ImplementAtion of energy Geostructure (FOLIAGE)”; PRIN2022 “Closing knowledge gaps on energy geostructures for retrofitting of buildings and infrastructures (GEOREFIT)”; CETP22FP-2022–00147 “Large-scale climate neutral Energy Geostructures in District Heating & Cooling systems/networks (LEG-DHC)”; The first author was partially supported by ERASMUS+.

Data Availability

Data will be made available on request.

References

1. Brandl H. Energy foundations and other thermo-active ground structures. *Géotechnique*. 2006;56(2):81–122.
2. Batini N, Rotta Loria AF, Conti P, Testi D, Grassi W, Laloui L. Energy and geotechnical behaviour of energy piles for different design solutions. *Appl Therm Eng*. 2015;85:199–213.
3. Ronchi F, Salciarini D, Cavalagli N, Tamagnini C. Thermal response prediction of a prototype Energy Micro-Pile. *GETE*. 2018;16:64–82. https://doi.org/10.1016/j.gete.2018.07.001.
4. Bourne-Webb P, Amatya B, Soga K, Payne P. Energy pile test at Lambeth College, London: geotechnical and thermodynamic aspects of pile response to heat cycles. *Géotechnique*. 2009;59(3):237–248.
5. Laloui L, Nuth M, Vulliet L. Experimental and numerical investigations of the behaviour of a heat exchanger pile. *Int J Numer Anal Methods Geomech*. 2006;30(8):763–781.
6. McCartney JS, Murphy KD. Strain distributions in full-scale energy foundations (DFI young professor paper competition 2012). *DFI J – J Deep Found Instit*. 2012;6(2):26–38. https://doi.org/10.1179/dfi.2012.008.
7. Murphy KD, McCartney JS. Seasonal response of energy foundations during building operation. *Geotech Geol Eng*. 2015;33(2):343–356.
8. Murphy KD, McCartney JS, Henry KS. Evaluation of thermo-mechanical and thermal behavior of full-scale energy foundations. *Acta Geotech*. 2015;10(2):179–195. https://doi.org/10.1007/s11440-013-0298-4.
9. Wang B, Bouazza A, Singh R, Haberfield C, Barry-Macaulay D. *Posttemperature Effects on Shaft Capacity of A Full-scale Geothermal Energy Pile. J Geotech Geoenviron Eng*. 2015, 04014125. https://doi.org/10. 1061/(ASCE)GT.1943-5606.0001266.
10. De Santiago C, de Santayana FP, De Groot M, et al. Thermo-mechanical behavior of a thermo-active precast pile. *Bulg Chem Commun*. 2016;48:41–54.
11. McCartney JS, Murphy KD. Investigation of potential dragdown/uplift effects on energy piles. *Geomech Energy Environ*. 2017;10:21–28.
12. Sutman M, Brettmann T, Olgun CG. Full-scale in-situ tests on energy piles: head and base-restraining effects on the structural behaviour of three energy piles. *Geomech Energy Environ*. 2019;18:56–68.
13. Faizal M, Bouazza A, Haberfield C, McCartney JS. Axial and radial thermal responses of a field scale energy pile under monotonic and cyclic temperatures. *J Geotech Geoenviron Eng*. 2018;144(10), 04018072.
14. Faizal M, Bouazza A, McCartney JS, Haberfield C. Axial and radial thermal responses of an energy pile under a 6-storey residential building. *Can Geotech J*. 2018. https://doi.org/10.1139/cgj-2018-0246.
15. Faizal M, Bouazza A, McCartney JS, Haberfield C. Effects of cyclic temperature variations on thermal response of an energy pile under a residential building. *J Geotech Geoenviron Eng*. 2019;145(10), 04019066.
16. Jiang G, Lin C, Shao D, et al. Thermo-mechanical behavior of driven energy piles from full-scale load tests. *Energy Build*. 2021;233, 110668. https://doi.org/10.1016/j.enbuild.2020.110668.
17. Ren Lw, Ren Jy, Han Zp, et al. Field tests on the thermomechanical responses of PHC energy piles under cooling and loading conditions. *Acta Geotech*. 2023;18:429–444.
18. Kong G, Li R, Deng H, Yang Q. Behaviours of a belled energy pile under heating-cooling cycles. *J Build Eng*. 2023;72, 106652.
19. Ng CWW, Shi C, Gunawan A, Laloui L. Centrifuge modelling of energy piles subjected to heating and cooling cycles in clay. *Géotech Lett*. 2014;4:310–316.
20. Stewart MA, McCartney JS. Centrifuge modeling of soil–structure interaction in energy foundations. ASCE. *J Geotech Geoenviron Eng*. 2014;140(4), 04013044-1-11.
21. Yavari N, Tang AM, Pereira J-M, Hassen G. Experimental study on the mechanical behaviour of a heat exchanger pile using physical modelling. *Acta Geotech*. 2014;9(3):385–398.
22. Goode III JC, McCartney JS. Centrifuge modeling of end-restraint effects in energy foundations. *J Geotech Geoenviron Eng*. 2015;141(8), 04015034-1-13.
23. Goode J.C., Zhang I.I.I.M., McCartney J.S. Centrifuge Modeling of Energy Foundations in Sand. In: Gaudin C, White D, eds. Physical Modeling in Geotechnics: Proc. 8th International Conference on Physical Modelling in Geotechnics. Perth, Australia. Jan. 14-17. Taylor and Francis: London; 2014, p. 729–736.
24. Goode III JC, McCartney JS. Evaluation of head restraint effects on energy foundations. In: Abu-Farsakh M, Hoyos L, eds. *Proc. GeoCongress 2014, GSP 234*. ASCE; 2014:2685–2694.
25. Ng CWW, Gunawan A, Shi C, Ma QJ, Liu HL. Centrifuge modelling of displacement and replacement energy piles constructed in saturated sand: a comparative study. *Geotech Lett*. 2016;6(1):34–38. https://doi.org/10.1680/ jgele.15.00119.
26. Yavari N, Tang AM, Pereira JM, Hassen G. Mechanical behaviour of a smallscale energy pile in saturated clay. *Geotechnique*. 2016;66(11):878–888.
27. Nguyen VT, Tang AM, Pereira J. Long-term thermo-mechanical behavior of energy pile in dry sand. *Acta Geotech*. 2017;12(4):729–737.
28. Vieira A, Maranha J. Thermoplastic analysis of a thermoactive pile in a normally consolidated clay. *Int J Geomech*. 2017;17(1), 04016030. https://doi.org/10.1061/(ASCE)GM.1943-5622.0000666.
29. Liu HL, Wang CL, Kong GQ, Bouazza A. Ultimate bearing capacity of energy piles in dry and saturated sand. *Acta Geotech*. 2019;14:869–879.
30. Yazdani S, Helwany S, Olgun G. Investigation of thermal loading effects on shaft resistance of energy pile using laboratory-scale model. *J Geotech Geoenviron Eng*. 2019;145(9), 04019043.1-04019043.12.
31. Ng CW, Farivar A, Gomaa SM, Jafarzadeh F. Centrifuge modeling of cyclic nonsymmetrical thermally loaded energy pile groups in clay. *J Geotech Geoenviron Eng*. 2021;147(12):04021146.
32. Zhao R, Leung AK, Knappett JA. Thermally induced ratcheting of a thermo-active reinforced concrete pile in sand under sustained lateral load. *Géotechnique*. 2022:1–14.
33. Golchin A, Guo Y, Vardon PJ, Liu S, Zhang G, Hicks MA. Shear creep behaviour of soil-structure interfaces under thermal cyclic loading. *Geotech Lett*. 2023:1–18.
34. Rafai M, Minh Tang A, Badinier T, Salciarini D, de Sauvage J. Thermally induced shear displacement of sand-concrete interface under different stress levels. *Symp Energy Geotech 2023*. 2023:1–2. https://doi.org/10.59490/seg.2023.541.
35. Rotta Loria AF, Gunawan A, Shi C, Laloui L, Ng CWW. Numerical modelling of energy piles in saturated sand subjected to thermomechanical loads. *Geomech Energy Environ*. 2015;1:1–15.
36. Chen, D.M. Soil Structure Interaction in Energy Piles Master thesis, Structural Engineering. University of California, San Diego, San Diego, CA, 2016.
37. Gawecka, et al. Numerical modelling of thermo-active piles in london clay. *ICE Geotech Eng*. 2017;170:201–219.
38. Knellwolf C, Peron H, Laloui L. Geotechnical analysis of heat exchanger piles. *J Geotech Geoenviron Eng*. 2011;137(10):890–902.
39. Salciarini D, Ronchi F, Tamagnini C. Thermo-hydro-mechanical response of a large piled raft equipped with energy piles: a parametric study. *Acta Geotech*. 2017;12:703–728. https://doi.org/10.1007/s11440-017-0551-3.
40. Rui Y, Yin M. Investigations of pile–soil interaction under thermomechanical loading. *Can Geotech J*. 2018;55(7):1016–1028. https://doi. org/10.1139/cgj-2017-0091.
41. Laloui L, Loria AFR. *Analysis and Design of Energy Geostructures: Theoretical Essentials and Practical Application*. Academic Press; 2019.
42. Ng CW, Zhao X, Zhang S, Ni J, Zhou C. An elasto-plastic numerical analysis of THM responses of floating energy pile foundations subjected to asymmetrical thermal cycles. *Géotechnique*. 2022:1–20.
43. Wu D, Liu H, Kong G, Li C. Thermo-mechanical behavior of energy pile under different climatic conditions. *Acta Geotech*. 2019;14:1495–1508.
44. NEN NPR 7201:2017 Geotechniek - Bepaling van het axiaal draagvermogen van funderingspalen door middel van proefbelasting (2017).
45. Fellenius B. From strain measurements to load in an instrumented pile. *Geotech N*. 2001;219(1):35–38.
46. Meibodi Saleh S, Loveridge Fleur. The future role of energy geostructures in fifth generation district heating and cooling networks. *Energy*. 2022;240, 122481.
47. Caulk R, Ghazanfari E, McCartney JS. Parameterization of a calibrated geothermal energy pile model. *Geomech Energy Environ*. 2016;5(3):1–15. https://doi.org/10.1016/j.gete.2015.11.001.
48. Abdelaziz SL, Ozudogru TY. Non uniform thermal strains and stresses in energy piles. *Environ Geotech*. 2016. https://doi.org/10.1680/jenge.15.00032.
49. Kong G, Fang J, Huang X, Liu H, Abuel-Naga H. Thermal induced horizontal earth pressure changes of pipe energy piles under multiple heating cycles. *Geomech Energy Environ*. 2021;26, 100228.
50. Fang J, Kong G, Yang Q. Group performance of energy piles under cyclic and variable thermal loading. *J Geotech Geoenviron Eng*. 2022;148(8), 04022060.
51. Lupattelli A, Salciarini D, Cecinato F, Veveakis M, Bodas Freitas TM, Bourne-Webb PJ. Temperature dependence of soil-structure interface behaviour in the context of thermally-activated piles: a review. *Geomech Energy Environ*. 2024, 100521.
52. Lupattelli A, Bourne-Webb PJ, Bodas Freitas TM, Salciarini D. A numerical study of the behavior of micropile foundations under cyclic thermal loading. *Appl Sci*. 2023;13(17):9791.
53. Rafai, M., Lupattelli, A., and Salciarini, D. 2022. FinitE Element Modelling of Energy Piles 740 usIng Different Constitutive Models for the Soil.
54. Bourne-Webb PJ, Lupattelli A, Freitas TMB, Salciarini D. The influence of initial shaft resistance mobilisation in the response of seasonally, thermally-activated pile foundations in granular media. *Geomech Energy Environ*. 2022;32, 100299.
55. Sittidumrong J, Jotisankasa A, Chantawarangul K. Effect of thermal cycles on volumetric behaviour of bangkok sand. *Geomech Energy Environ*. 2019, 100127. https://doi.org/10.1016/j.gete.2019.100127.
56. Lupattelli A, Cernuto E, Brunelli B, Cattoni E, Salciarini D. Experimentation of the thermo-mechanical behavior of the soil-concrete interface. *Springe Ser Geomech Geoeng*. 2023:343–350.
57. Rafai, M., Salciarini, D., Vardon, P.J. Thermo-Mechanical Response of A Cast in Situ Displacement Energy Pile; EGU General Assembly, Vienna, Austria, 14–19 Apr 2024, EGU24-7965, 743 https://doi.org/10.5194/egusphere-egu24-7965, 2024.
58. Guo Y, Golchin A, Hicks MA, et al. Experimental investigation of soil–structure interface behaviour under monotonic and cyclic thermal loading. *Acta Geotech*. 2023;18:3585–3608. https://doi.org/10.1007/s11440-022-01781-5.
59. Jiang G, Shao D, Zong C, et al. Thermo-mechanical behavior of long-bored energy pile: a full-scale field investigation. *KSCE J Civ Eng*. 2023;27(1):145–155.
60. Rafai M, Tang AM, Badinier T, de Sauvage J, Salciarini D. Effect of thermal cycles on sand-concrete interface under constant shear stress. *Can Geotech J*. 2024. https://doi.org/10.1139/cgj-2023-0140.
61. Morteza Zeinali S, Abdelaziz SL. Thermal consolidation theory. *J Geotech Geoenviron Eng*. 2021;147(1), 04020147.